THE COOPER UNION FOR THE ADVANCEMENT OF SCIENCE AND ART
ALBERT NERKEN SCHOOL OF ENGINEERING

Joint Spatial-Temporal Equalization of 3G HF Communications

by

Samantha G. Massengill

A thesis submitted in partial fulfillment
of the requirements for the degree of
Master of Engineering

September 3, 2013

Advisor

Dr. Sam M. Keene

THE COOPER UNION FOR THE ADVANCEMENT OF SCIENCE AND ART
ALBERT NERKEN SCHOOL OF ENGINEERING

This thesis was prepared under the direction of the Candidate's Thesis Advisor and has received approval. It was submitted to the Dean of the School of Engineering and the full Faculty, and was approved as partial fulfillment of the requirements for the degree of Master of Engineering.

Dr. Teresa A. Dahlberg
Dean, School of Engineering

Dr. Sam M. Keene
Candidate's Thesis Advisor

Acknowledgments

Thank you to Sam Keene for his patience and guidance; to Glen Mabey for his mentorship, encouragement, and friendship; to Ryan Casey and Jason Polendo for their willingness to share time and expertise; to my parents for their love, support, and understanding; to my friends for showing me what it means to truly be part of a community; to Bryan for joyfully, lovingly, and tirelessly supporting me and encouraging me in every way he knows how; and to God for sustaining me and giving me strength.

Abstract

The high frequency (HF) spectrum is home to many military communication signals that rely on receivers to accurately equalize, demodulate, and decode signals of interest. This is not a trivial task when faced with the challenges that arise from signals being reflected back to Earth by the ionosphere. To combat HF channel effects, it is desirable to exploit spatial diversity; however, the design of diversity receivers becomes complicated especially when limited channel information is available.

This work describes the design and testing of an HF military standard (MIL-STD) 188-141B (ALE3G) diversity receiver that uses a joint spatial-temporal equalizer to perform the dual task of combining and equalizing the signals received by multiple antennas prior to demodulation and decoding of transmitted data. The receiver requires no prior knowledge of the channel, array geometry, or angle of arrival of the multipath signal. This design is evaluated against two diversity receivers that perform linear combining followed by single-channel equalization. For various adaptive filter parameters, the joint spatial-temporal equalizer has a shorter convergence time and lower mean squared error (MSE) than the combiner and equalizer. At low SNRs, the spatial-temporal equalizer also outperforms in terms of bit error rate (BER), showing up to a 10 dB improvement over the single-channel equalizer structure.

Contents

List of Figures

List of Tables

Chapter 1

Introduction

1.1 Motivation

Over the past decade, high frequency (HF) radio communications have witnessed a period of renewal, largely due to the advances of third-generation (3G) and wideband HF (WBHF) technologies [13]. Due to increasing popularity amongst military and governmental communities, this thesis focuses on improving the reception of 3G automatic link establishment (ALE3G) tranmissions. Oftentimes, reception of ALE3G signals is done by a third party for whom the transmitted message was not originally intended. In addition to HF radio receivers having to overcome ionospheric channel effects, there are additional challenges that the passive listener faces which do not exist for cooperative receivers; for example, the receiver may require additional information from the transmitter in order to perform timing synchronization, demodulation, or decoding. Furthermore, the channel quality is potentially worse for a passive listener since he may be hundreds of kilometers away from the cooperative receiver. This thesis addresses the need for improved receivers in the presence of HF channel effects, particularly when minimal information is available to the receiver.

1.2 Problem Statement

There are multiple ways in which a signal propagating through an HF channel can be distorted. If copies of the signal are delayed in time and this delay is on the order of one symbol period, intersymbol interference (ISI) can occur as a result. In a digital communications system, equalizers are used to mitigate ISI by creating a filter that estimates the inverse of the channel and then passing the ISI-corrupted signal through the filter to recover the original transmitted message.

In addition to equalization, the reliability of receiving a multipath signal can improve greatly with the use of receiver diversity. For a time-varying channel with fading, using more than one receive antenna is useful since it is unlikely that each antenna will be experiencing the same fading. The goal of this work is to introduce a spatial-temporal equalizer that jointly performs equalization and diversity combining in an HF channel. Possible benefits of introducing this scheme include the receiver requiring less channel state information, lower computational complexity, better performance under certain conditions, and reducing the need for additional components in a modular software-defined radio dataflow architecture.

1.3 Previous Work

There has been a substantial amount of research done in investigating combined spatial-temporal equalization for digital communications systems. In [15], suboptimal solutions to spatial-temporal decision feedback equalization were investigated in hopes of greatly reducing computational complexity while still preserving good performance. The authors compare three algorithms: the general beam decision feedback equalizer (GB-DFE), the multiple independent beam decision feedback equalizer

(MIB-DFE), and simultaneous beamforming and equalization iterating with the LS-algorithm (SBE-LS). The GB-DFE is simply a MISO FIR decision feedback equalizer where the signals from each array are delayed and summed before equalization. The MIB-DFE, proposed by the authors, performs optimization on antenna weights prior to equalization where the combiner weights and equalizer weights are optimized using two different criteria. The last algorithm, SBE-LS, also proposed by the authors, optimizes beamformer weights and equalizer coefficients using two RLS filters. The algorithm is first applied to the equalizer coefficients while holding the beamformer weights fixed, then applied to the beamformer weights while equalizer coefficients are fixed. It is shown that for short training sequences, the MIB-DFE outperforms the other two algorithms and requires the least number of computations.

In [8], it is shown that a joint space-time DFE (ST-DFE) is superior to a structure having a preselection diversity switch followed by a temporal DFE for frequency-selective cellular fading channels. For the ST-DFE, the authors use a QR-decomposition type of RLS algorithm for the weight adaptation due to its efficient and stable implementation.

In [7], antenna combiner weights and equalizer weights are jointly optimized but remain separate entities. Typically, the combiner chooses its weights prior to symbol detection and does not have access to the newest information available. The authors design an equalizer-assisted combiner, where the error from the equalizer is fed back to help the combiner adjust its weights after symbol decisions have been made. The combiner optimization is performed using the LMS algorithm. A second algorithm is proposed that jointly minimizes the output cluster variance by using LMS to adapt the equalizer weights and "filtered-X LMS" to adjust the combiner weights.

In [10], a spatial-temporal equalizer has been simulated using an adaptive tapped

delay line antenna array and the Zero-Forcing algorithm and it was shown that this system outperforms conventional temporal equalization. In [4], a multiple-input adaptive combiner-equalizer is designed by adding tapped delay lines at each diversity branch and then feeding the delayed signals to the inputs of a linear neuron whose weights are updated using LMS or RLS. The authors show that replacing a maximal-ratio combiner and linear equalizer with a neural network yields results that are comparable in performance but much less complex to implement especially on software defined ratio (SDR) platforms.

Much work has also been done in simulating HF transmissions and proposing enhancements to improve ALE3G reception. Simulations of MIL-STD-188-141B Appendix C, a US Department of Defense standard for HF radio where ALE3G is defined, and STANAG 4538, a NATO standard that also defines ALE3G, are documented in [25], [2], [14], [11], [12], [23] and proposed enhancements to STANAG 4538 are suggested in [1]. Most of these simulations assume a single-channel receiver and minimal research has been done in spatial diversity for HF communications. In [17], multisite combination is performed to improve demodulation of HF signals. The signals are transmitted in Texas and received in Utah and Maryland, so receiving antennas are separated too far apart to constitute spatial diversity. The author mentions joint spatial-temporal equalization as a possibility for future work on HF demodulation. In [5], blind spatial-temporal equalization in HF is developed using the Constant Modulus Algorithm (CMA) on a polarization sensitive array of four collocated antennas wherein spatial-temporal equalization improves performance significantly over the single-channel case.

1.4 Proposed Solution

The algorithm most similar to the one actually implemented in this thesis is presented in [22]. The authors use spatial diversity equalization to improve reliability of underwater communications. Each channel is linearly equalized and the outputs are combined using an adaptive multi-channel combiner driven by the RLS algorithm. The combiner input signals from all diversity channels are concatenated together to form a single composite input signal and similarly, a composite tap-weight vector is what is updated during the RLS optimization.

This idea is extended for HF communications. Instead of equalizing each channel prior to combining, these operations are done simultaneously such that the equalizer weights and combiner weights are optimized jointly. The RLS filter composite input vector and composite tap-weight vector are formed similarly as in [22] such that each iteration of the RLS algorithm contains both temporal and spatial information. After the algorithm is developed, it is tested against a more traditional receiver that first combines and then equalizes.

The rest of the thesis is outlined as follows. Chapter 2 discusses an overview of HF communications, the ionosphere and how to simulate its behavior using the Watterson model, and MIL STD 188-141B (ALE3G), the standard implemented for use in the simulations presented in this work. Chapter 3 gives an overview of equalization, followed by summaries of the LMS and RLS adaptive filtering algorithms used for adaptive equalization in this thesis. Next, Chapter 4 illustrates the basic principles and advantages of receiver diversity by first giving a brief overview of diversity techniques and then focusing on spatial diversity and combining methods. Chapter 5 introduces the joint spatial-temporal equalizer developed in this work and describes the simulation platform. Chapter 6 presents and discusses experimental results, and

Chapter 7 draws conclusions and suggests possible avenues for future work.

Chapter 2

HF Communications

2.1 Introduction to HF

High frequency (HF) radio waves are transmitted in the 3-30 MHz range and have wavelengths of 200 m or less. Due to these relatively short wavelengths, HF radio was originally overlooked for commercial use despite many desirable characteristics when compared to longer wavelength radios. For example, global ranges can be attained in the HF band with less power than longer wavelength radios and HF antennas are easier to build. Satellite communications also achieve global ranges but require additional infrastructure making them less cost efficient than HF networks. Therefore, it is common to see HF radio used as a backup for satellite communications [13].

2.2 The Ionosphere

HF radio is able to achieve global ranges due to waves refracting off the ionosphere as shown in Figure 2.1 where a man receives signals that traveled to him via two different paths. This is an example of skywave propagation where signals are launched

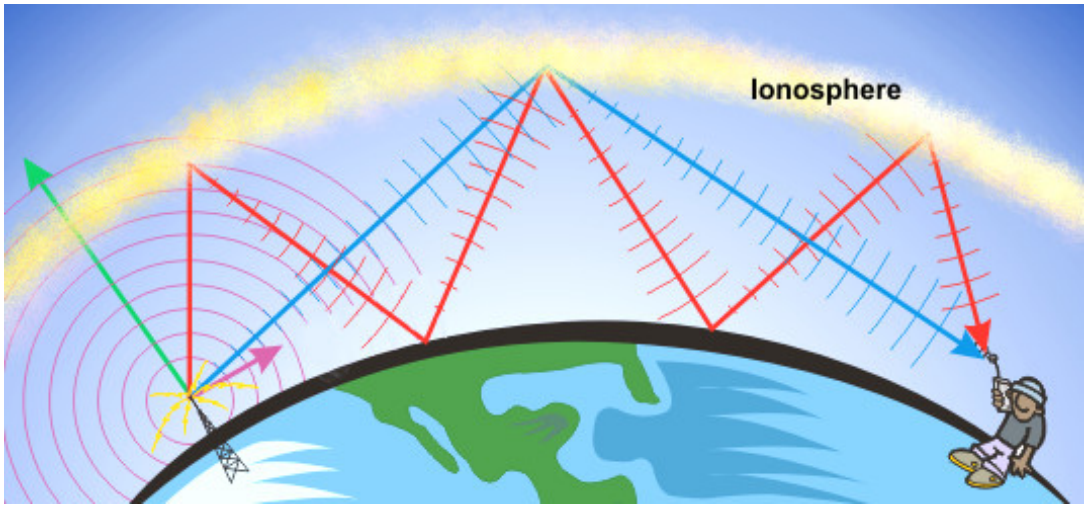

Figure 2.1: Ionospheric refraction [3]

skyward and are bounced back and forth between the Earth and the ionosphere. In addition to skywaves, there exist surface waves and space waves in HF but neither of these interact with the ionosphere. Surface wave propagation refers to signals that travel near the Earth's surface following its curvature such that over-the-horizon ranges can be reached but not global ranges. Space waves are either line-of-sight (direct) transmissions or signals that are reflected off the Earth's surface [3]. Skywaves are more widely studied in HF channels due to the long distances these transmissions can travel.

The ionosphere is a region of the atmosphere that has an abundance of free electrons due to solar radiation and cosmic rays that ionize the air. The density of free electrons and of gas molecules to be ionized varies with altitude. There are three layers of the ionosphere: D layer, E layer, and F layer, in increasing distance from the Earth. Due to the lowest level of ionizing radiation being the furthest from the Sun, the D layer has a low electron density and high neutral gas density. The E layer has higher electron density and lower neutral gas density, and the highest electron

density and lowest neutral gas density are found in the F layer at approximately 300 km above the Earth's surface. The F layer has an additional layer during the day due to solar radiation, where the F1 layer is between the E layer and the F2 layer and the F2 layer is simply referred to the F layer at night. When a wave interacts with the ionosphere, the wave is refracted according to the ionosphere's free electron density and the wave's frequency; a higher frequency will result in decreased refraction [13].

In addition to the unpredictable nature of the ionospheric channel as a result of its dependence on solar activity, there exist losses in signal strength associated with reflection and refraction. Additionally, fading in both time and frequency make the HF channel even more cumbersome to deal with. Due to the dispersive nature of the ionosphere, multiple copies of a single transmitted signal arrive at a receiver. The different paths taken by the signal are each different lengths and therefore also have different phases. This multipath propagation could cause intersymbol interference due to spreading in time and multipath fading due to shifts in frequency. Other potential causes of fading are the Faraday effect and ray interference [13]. These channel impairments create many challenges for engineers who make HF modems and so there is a need for standardized channel models that are used for testing of such modems.

2.3 Watterson Model

The widely accepted mathematical model used for HF testing is the Watterson model [24]. The Watterson model assumes the signal travels as two paths, each having equal losses and separated by a fixed differential time delay. At the receiving antennas, additive white Gaussian noise (AWGN) is added to simulate thermal noise. The model also assumes a Doppler spread which is a fading-gain process with

Table 2.1: ITU-R F.1487 Ionospheric Channel Parameters [20]

Channel condition	Delay spread (ms)	Doppler spread (Hz)
Low latitude, quiet	0.5	0.5
Low latitude, moderate	2	1.5
Low latitude, disturbed	6	10
Mid-latitude, quiet	0.5	0.1
Mid-latitude, moderate	1	0.5
Mid-latitude, disturbed	2	1
Mid-latitude, disturbed NVI	7	1
High latitude, quiet	1	0.5
High latitude, moderate	3	10
High latitude, disturbed	7	30

a specified bandwidth. The ITU-R recommendation for Watterson channel simulator representative values are shown in Table 2.1. Near vertical incidence (NVI) occurs when a signal is sent almost straight up such that it is refracted back to a nearby receiver that is separated from the transmitter by a physical obstruction. Engineers who use the Watterson model to simulate HF channels must specify the delay spread, Doppler spread, and SNR for their model.

2.4 MIL-STD-188-141B

Automatic link establishment (ALE) describes the process of finding and managing an HF frequency for voice and data (email, texting, file transfer, etc.) traffic. To combat increasing congestion in the HF band during the mid-1990's and improve spectrum efficiency, a third generation automatic link establishment (ALE3G) standard was designed and described in the US Department of Defense MIL-STD-188-141B Appendix C. ALE3G is also part of STANAG 4538, a NATO implementation that includes additional capabilities not originally presented in MIL-STD-188-141B Appendix C. ALE3G is an 8-level PSK serial-tone waveform modulated onto an 1800 Hz

carrier with a baud rate of 2400 symbols per second. Like most other HF communications signals, ALE3G is filtered to a 3-kHz bandwidth and uses single-sideband mode of operation.

The physical layer of ALE3G is manifested as "burst waveforms"; to date, there are six of these waveforms that have been defined in standards [21], [18]: BW0, BW1, BW2, BW3, BW4, BW5, and a seventh, BW1+, which is a proprietary burst waveform developed by Harris Corporation [1] and has been proposed as an enhancement to the standard. Only two of these waveforms, BW2 and BW3, send data traffic (of varied duration), while the remaining BWs are used for shorter transmissions (fixed duration) such as acknowledgements (ACKs), link establishment, link management, network time synchronization, and channel probing.

Generally, the structure of each burst waveform has three sections of PN-spread 8-ary PSK symbols. The first section is the transmit level control (TLC), followed by an acquisition preamble, and ending with a data section. The purpose of the TLC section is to give the system enough time for its transmitter TLC and receiver automatic gain control (AGC) to adjust and stabilize. The preamble section contains a different sequence of symbols that are unique to each different burst waveform in terms of the order of symbols, the duration of the preamble, or both the order and duration. Each burst waveform also has a different payload duration and structure. In general, burst waveforms undergo error correction coding, interleaving, symbol formation, and PN spreading before they are modulated and transmitted. Unlike the rest of the waveforms, BW2 does not use Walsh symbol formation and instead forms symbols using a series of rotation, gray coding, and frame formation. See Figure 2.2 for a summary of burst waveform characteristics, excluding the proprietary BW1+.

To introduce redundancy, the payload bits for the burst waveforms that carry

Wave Form	*Used for*	*Burst Duration1*	*Payload*	*Preamble*	*FEC Coding*	*Interleaving*	*Data Format*	*Effective Code Rate2*
BW0	Robust LSU PDUs	613.33 ms 1472 PSK symbols	26 bits	160.00 ms 384 PSK symbols	Rate = 1/2, k = 7 convolutional (no flush bits)	4x13 block	16-ary Walsh function	1/96
BW1	Traffic management PDUs; HDL Ack PDUs	1.30667 seconds 3136 PSK symbols	48 bits	240.00 ms 576 PSK symbols	rate = 1/3, k = 9 convolutional (no flush bits)	16x9 block	16-ary Walsh function	1/144
BW2	HDL traffic data PDUs	126.67 + (n*400) ms 304 + (n*960) PSK symbols, n = 3, 6, 12, or 24	n*1881 bits	26.67 ms 64 PSK symbols (for equaliser training)	rate = 1/4, k = 8 convolutional (7 flush bits)	None	32 unknown/ 16 known	variable: 1/1, 1/2, 1/3, 1/4, ...
BW3	LDL traffic data PDUs	373.33 + (n*13.33) ms	8n+25 bits	266.67 ms 640 PSK symbols	rate = 1/2, k = 7 convolutional (7 flush bits)3	convolutional block	16-ary Walsh function	variable: 1/12, 1/24, ...
BW4	LDL acknowledg-ment PDUs	640.00 ms	2 bits	None	None	None	4-ary Walsh function	1/1920
BW5	Fast LSU PDUs	1.01333 seconds 2432 PSK symbols	50 bits	240.00 ms	Rate = 1/2, k = 7 convolutional (no flush bits)	10x10 block	16-ary Walsh function	1/96

1. All transmissions begin with a TLC/AGC guard sequence (part of the preamble for BW3). These symbols are included in the indicated burst durations.
2. Reflects forward error correction (FEC) and Walsh-function coding only, relative to uncoded 8-PSK; does not include known data or convolutional encoder flush bits.
3. In this case, the number of flush bits exceeds by one the minimum number required to flush the convolutional encoder; this makes the number of coded bits a multiple of four as is required for the Walsh-function modulation format.

Figure 2.2: Burst waveform characteristics [13]

data information (BW2 and BW3) are encoding using convolutional encoding with flush bits that are known to the receiver. For short burst waveforms (all but BW2 and BW3), the bits are encoded using tail-biting convolutional encoding. Tail-biting ensures that the initial state of the encoder is the same as the final state so that the use of flush bits is not necessary. The reason for this is to save additional overheard that would be needed to transmit flush bits because for short payloads, the flush bits could amount to a significant percentage of the total transmit bits.

After the data bits are convolutionally encoded, they are interleaved using either a block interleaver or a convolutional block interleaver structure. The purpose of this

step is to spread out potential bursts of errors. The pseudo-code for filling and fetching from the interleave matrix can be found in [18], [21]. For BW0, BW1, and BW5, the deinterleave matrix is a simple matrix transpose of the interleave matrix.

With the exception of BW2, data bits are modulated using an orthogonal Walsh function. In groups of either four or two bits, the bits are mapped to 16 symbols of 0s and 4s. For BW0, BW1, and BW5, the tribit sequences in Figure 2.5 are repeated four times per four coded bits. For BW3, the sequences are not repeated and for BW1+ the sequences are repeated twice. BW4 maps two bits (00,01,10,11) to only the first four tribit sequences in Figure 2.5 and each sequence is repeated 80 times. The symbols are then added modulo-8 to a pseudo-noise (PN) scrambling sequence which is essentially the mapping of a BPSK signal to an 8-PSK signal prior to transmission. On the demodulation side, this step involves descrambling an 8-PSK signal to a BPSK signal, as shown in 2.3.

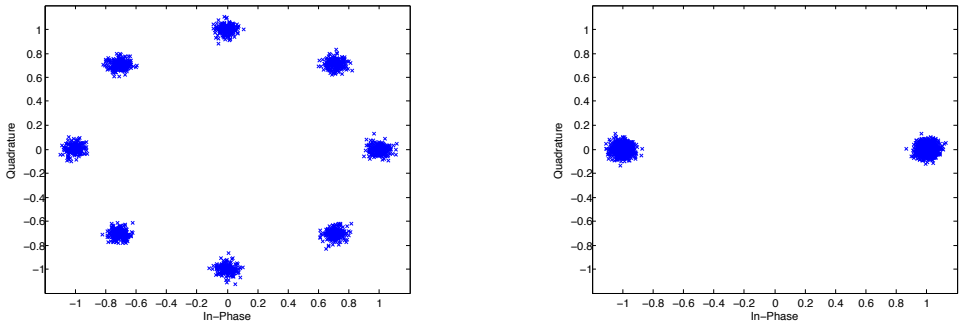

(a) Raw symbols out of equalizer

(b) Descrambled symbols

Figure 2.3: BW5 descrambling, SNR 30 dB

As an example, BW5 is discussed here in more detail. BW5 is an extended and more robust verison of BW0, both of which are used for link setup at the beginning of an ALE3G exchange. As shown in Figure 2.4, BW5 begins with a 256-symbol TLC/AGC guard sequence, followed by 576 preamble symbols and 1600 payload sym-

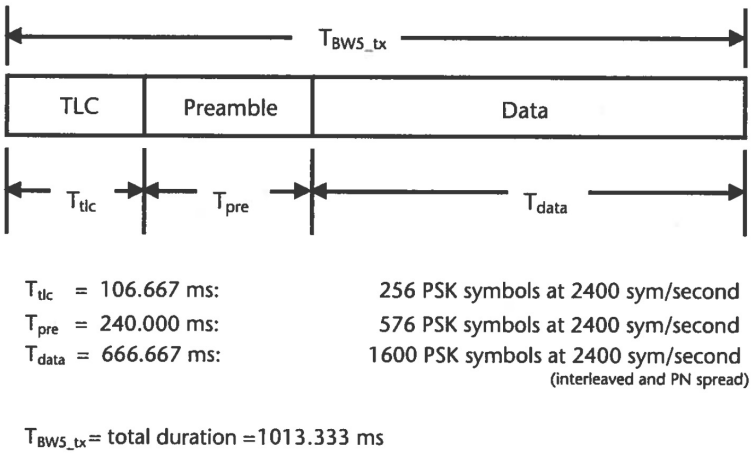

Figure 2.4: BW5 structure [13]

Coded Bits (shown as $\mathbf{b_3b_2b_1b_0}$)	Tribit Sequence
0000	0000 0000 0000 0000
0001	0404 0404 0404 0404
0010	0044 0044 0044 0044
0011	0440 0440 0440 0440
0100	0000 4444 0000 4444
0101	0404 4040 0404 4040
0110	0044 4400 0044 4400
0111	0440 4004 0440 4004
1000	0000 0000 4444 4444
1001	0404 0404 4040 4040
1010	0044 0044 4400 4400
1011	0440 0440 4004 4004
1100	0000 4444 4444 0000
1101	0404 4040 4040 0404
1110	0044 4400 4400 0044
1111	0440 4004 4004 0440

Figure 2.5: Walsh modulation of coded bits to tribit sequences [18]

bols. The payload, consisting of 50 protocol bits, are encoded using a $r = 1/2$, $k = 7$ tail-biting convolutional encoder with polynomials $b_0 = x^6 + x^4 + x^3 + x^1 + 1$ and $b_1 = x^6 + x^5 + x^4 + x^3 + 1$ as seen in Figure 2.6. After encoding, the 100 bits are interleaved using a 10x10 block interleaver. Each group of four coded and interleaved bits are mapped to a tribit sequence (Figure 2.5) repeated four times resulting in 64

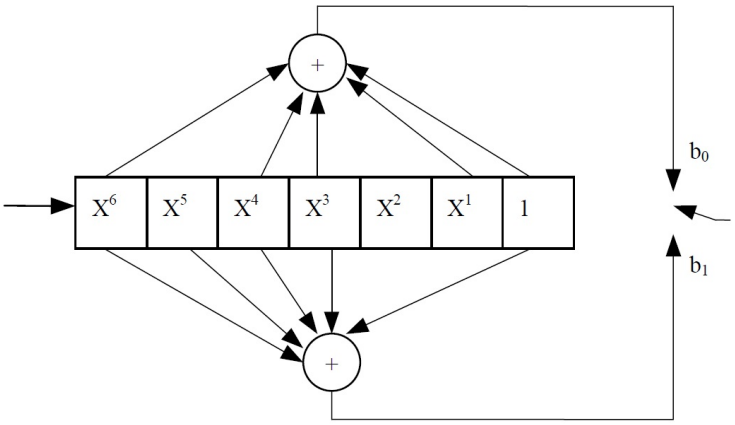

Figure 2.6: BW5 convolutional encoder [21]

symbols for every four coded bits or 1600 total payload symbols; these symbols are then component-wise modulo-8 added to a PN sequence and modulated onto an 1800 Hz carrier signal.

ALE3G is a complicated signal which includes many stages of redundancy due to the challenges that must be overcome when transmitting through the ionosphere. While redundancy is certainly helpful, the following chapters explain how adaptive equalization and spatial diversity are also important tools that can be used to demodulate and decode a reliable ALE3G signal.

Chapter 3

Adaptive Equalization

3.1 Basics of Equalization

In a digital communications system, time dispersion is caused when data passes through any frequency-selective channel. The amount of time dispersion and its cause varies amongst transmission systems, but higher-data-rate applications such as those described in Chapter 2 are most susceptible to delay spread. If the delay spread is significant enough, pulses will be distorted such that zero-crossings will no longer be periodic due to adjacent pulses overlapping. This phenomenon is called intersymbol interference (ISI). To mitigate the effects of ISI caused by a dispersive channel, an equalizer can be used to model the inverse of the channel and restore pulses.

Because wireless communication channels typically vary in time, the filter coefficients for the equalizer may also be time-varying. If this is the case, an adaptive equalizer is necessary so that tap weights can be adjusted adaptively and the equalizer can best approximate the time-varying channel response inversion in real time. Typically, there is a training sequence at the beginning of a transmission where known symbols are sent and the equalizer adjusts its filter parameters by comparing its output

to the known data. After the training sequence ends, the equalizer will leave training mode and enter decision directed mode (also sometimes called tracking mode) where the equalizer will have to make its own decisions based on what its learned from previous decisions made during training. Two adaptive filtering algorithms commonly used in practice to adjust filter coefficients are the least-mean-square (LMS) and recursive least-squares (RLS) algorithms which are both described in the next two sections of this chapter.

Equalizers can be linear or non-linear. Non-linear equalizers, such as decision feedback equalizers (DFE) or maximum likelihood sequence estimation (MLSE), are more complex to implement but are better at reducing noise enhancement. This thesis focuses on linear equalizers due to their simplicity but Chapter 7 mentions the possibility of a DFE in future implementations of the joint spatial-temporal equalizer algorithm. Linear equalizers can be implemented using either a transversal or lattice structure, but the focus of this thesis is on transversal filters. Linear equalizers can either be zero-forcing (ZF) equalizers or minimum mean square error (MMSE) equalizers; ZF equalizers apply the inverse of the channel's frequency response and reduce ISI completely at the expense of enhancing noise, and MMSE equalizers aim to minimize the error between the desired response and the actual response of the equalizer. This thesis focuses on MMSE equalization.

It should be noted that a fractionally spaced equalizer is an equalizer that receives an oversampled signal such that the output sample rate is K/T where K is an integer corresponding to the number of input samples the equalizer received before producing a single output sample. There are advantages to fractionally spaced equalizers when the receiver does not know channel characteristics [19], however, as a simplification, the focus of this work is on symbol-spaced equalization where the equalizer input and

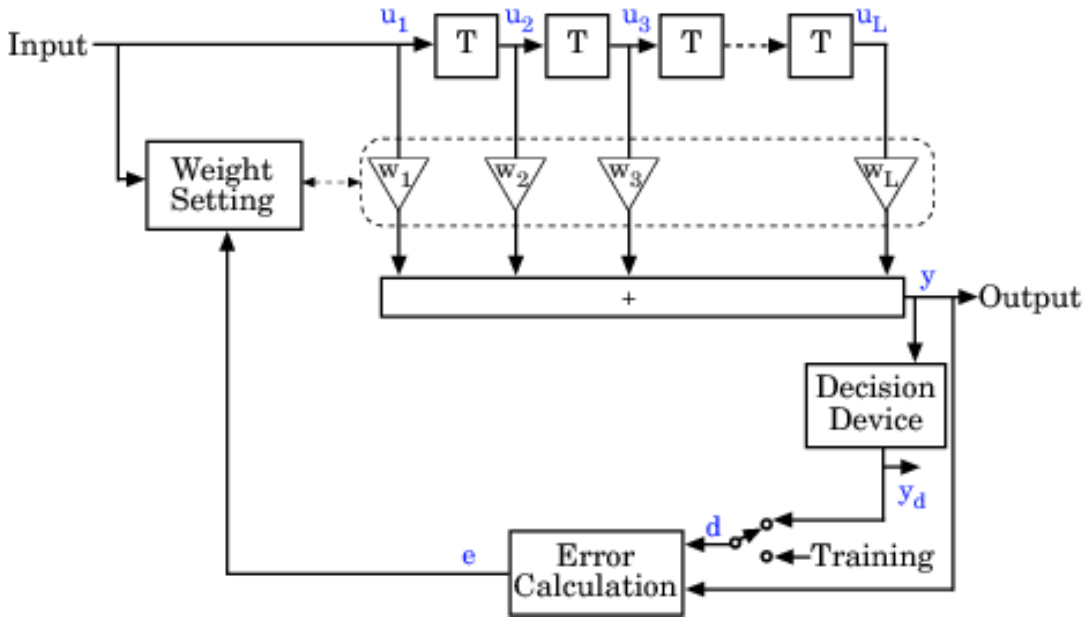

Figure 3.1: Symbol-spaced linear equalizer [16]

output sampling rates are equal.

Figure 3.1 shows the general structure for a symbol-spaced equalizer consisting of a tapped delay line with $L-1$ delay elements, L tunable complex weights, an adaptive weight setting, decision device, and error calculator.

To quantify equalizer performance, the mean squared error (MSE) is plotted against each iteration of the algorithm in time, or, the number of training symbols. The MSE is in terms of the Euclidean distance between the desired symbol and the actual symbol. These curves are called learning curves because they show how quickly the equalizer is learning the channel and the learning rate is referred to as the rate of convergence. In addition to convergence time, the value of the MSE to which the equalizer converges can be used to show how well an equalizer is doing. Another useful way to check equalizer performance is to plot the output symbols. For a PSK signal, a constellation where each phase is tightly clustered together will imply that

the equalizer is working well.

3.2 LMS Filtering

The least-mean-square (LMS) algorithm is a type of stochastic gradient descent algorithm [9]. Its feedback structure is a linear transversal (FIR) filter whose tap weights are updated by an adaptive weight-control mechanism driven by minimizing a cost function. For a Wiener filter, the cost function to be minimized is the mean squared error:

$$J(n) = E[e(n)e^*(n)] \tag{3.1}$$

where the error signal $e(n)$ is computed by comparing the filter output with a desired response. If parameters are chosen appropriately, the LMS algorithm will converge to an estimate of the optimum Wiener solution. Since the gradient vector $\nabla J(n)$ at each iteration of the steepest-descent algorithm is only an estimate, LMS will only approach the optimal solution. Therefore, the cost function for LMS becomes the instantaneous squared error:

$$J(n) = |e(n)|^2 \tag{3.2}$$

The LMS algorithm solves for the optimum value of the tap-weight vector $\hat{\mathbf{w}}(n+1)$ that minimizes the cost function $J(n)$. Using the notation, approximations, and steepest descent method results described in [9], we summarize the algorithm as follows. First, the tap-weight vector is initialized:

$$\hat{\mathbf{w}}(0) = \mathbf{0} \tag{3.3}$$

An L-by-1 tap-input vector at time n is given:

$$\mathbf{u}(n) = [u(n), u(n-1), ..., u(n-L+1)]^T \tag{3.4}$$

where L is the length of the adaptive transversal filter. Also given is the desired response d(n) at time n. For an adaptive equalizer, the desired response is usually a training sequence or probes known to the receiver. Next, an estimate of the tap-weight vector at time $n+1$ is computed using the system:

$$e(n) = d(n) - \hat{\mathbf{w}}^H(n)\mathbf{u}(n) \tag{3.5}$$

$$\hat{\mathbf{w}}(n+1) = \hat{\mathbf{w}}(n) + \mu\mathbf{u}(n)e^*(n) \tag{3.6}$$

where μ is the step size parameter, a small positive quantity. At each iteration, the LMS algorithm requires only $2L+1$ multiplications; it is a simple but powerful tool.

3.3 RLS Filtering

The recursive least-squares (RLS) algorithm is another method used to recursively estimate the tap-weight vector of a linear transversal filter. Unlike LMS, it is an extension of the method of least squares rather than a stochastic gradient descent approach. At the cost of computational complexity, the RLS algorithm converges significantly faster (usually by an order of magnitude) than the LMS algorithm [9]. The RLS cost function to be minimized is:

$$\varepsilon(n) = \sum_{i=1}^{n} \lambda^{n-i}|e(i)|^2 + \delta\lambda^n\|\mathbf{w}(n)\|^2 \tag{3.7}$$

where the first term of the cost function is the sum of exponentially weighted error squares. The exponential weighting is due to the forgetting factor λ^{n-i} where λ is a positive constant less than but close to 1 and serves as a measure of the algorithm's memory for past data. Similar to LMS, the error is defined as the difference between the desired response and the actual response of the filter:

$$e(i) = d(i) - \mathbf{w}^H(n)\mathbf{u}(i) \tag{3.8}$$

where the tap-input vector and tap-weight vectors are defined by

$$\mathbf{u}(i) = [u(i), u(i-1), ..., u(i-L+1)]^T \tag{3.9}$$

$$\mathbf{w}(n) = [w_0(n), w_1(n), ..., w_{L-1}(n)]^T \tag{3.10}$$

Note that only the tap weights remain fixed during the time interval. The second term of the cost function is referred to as the regularizing term since the regularizing parameter δ is a positive real number included in the cost function for stability and smoothing.

The RLS algorithm minimizes the cost function $\varepsilon(n)$ by using a reformulation of the correlation matrix of the tap-input vector $\mathbf{u}(i)$ to compute the tap-weight estimate $\hat{\mathbf{w}}(n)$. In order to do this computation, the matrix inversion lemma is used to calculate the inverse of the correlation matrix, $\mathbf{P}(n) = \mathbf{\Phi}^{-1}(n)$. Using the notation, approximations, method of least-squares results, and matrix inverse lemma results described in [9], we summarize the algorithm as follows. In similar fashion to the LMS algorithm, the tap-weight vector is first initialized in addition to the inverse correlation matrix:

$$\hat{\mathbf{w}}(0) = \mathbf{0} \tag{3.11}$$

$$\mathbf{P}(0) = \delta^{-1}\mathbf{I} \tag{3.12}$$

At every time instant, the following equations are computed:

$$\boldsymbol{\pi}(n) = \mathbf{P}(n-1)\mathbf{u}(n) \tag{3.13}$$

$$\mathbf{k}(n) = \frac{\boldsymbol{\pi}(n)}{\lambda + \mathbf{u}^H(n)\boldsymbol{\pi}(n)} \tag{3.14}$$

$$\xi(n) = d(n) - \hat{\mathbf{w}}^H(n-1)\mathbf{u}(n) \tag{3.15}$$

$$\hat{\mathbf{w}}(n) = \hat{\mathbf{w}}(n-1) + \mathbf{k}(n)\xi^*(n) \tag{3.16}$$

$$\mathbf{P}(n) = \lambda^{-1}\mathbf{P}(n-1) - \lambda^{-1}\mathbf{k}(n)\mathbf{u}^H(n)\mathbf{P}(n-1) \tag{3.17}$$

where $\mathbf{k}(n)$ is the gain vector, $\xi(n)$ is the a priori estimation error computed during the filtering operation, $\hat{\mathbf{w}}(n)$ is the estimated tap-weight vector update, and the inverse correlation matrix $\mathbf{P}(n)$ is used to update the gain vector. The biggest downfall of the RLS algorithm is its computational complexity: it requires $2.5L^2+4.5L$ multiplications per iteration [6].

In summary, the LMS and RLS algorithms are powerful algorithms that can control the weight adaptation for adaptive equalization of signals blurred together from ISI. The RLS algorithm converges much faster than LMS but is more complex to implement. Both algorithms with varying parameters are used for the simulations described later in Chapter 5.

Chapter 4

Receiver Diversity

4.1 Basics of Diversity

In a fading channel, it is unlikely that multiple independent signal paths will all experience a deep fade at the same time [6]. Therefore, it is desirable to create a situation in which the same data is being sent over multiple independent paths because adding these signals together results in a higher SNR than the SNR from a single path. Independent fading paths can be obtained in a number of ways. Spatial diversity refers to a situation where there are multiple transmit or receive antennas, where maximum diversity gain is achieved by separating antennas by approximately one half-wavelength if the antennas are omnidirectional [6]. Other diversity techniques include polarization diversity (where two antennas have vertical and horizontal polarizations), directional diversity (by use of directional antennas that specify a particular receive beamwidth), and frequency diversity (by transmitting at different carrier frequencies). The focus of this thesis is on receiver spatial diversity so the combining techniques described in the following sections will be discussed in such a context. Spatial diversity was chosen because of the popularity of multi-channel HF receivers.

4.2 Combining Techniques

The general structure for a linear combiner is illustrated in Figure 4.1. The complex weights α_i are used to scale each of the received signals $r_i e^{j\theta_i} s(t)$ where $s(t)$ is the transmitted signal, r_i is the amplitude of the signal at the ith branch, and θ_i is the phase of the signal at the ith branch. Depending on the combining technique, α_i will take on different forms. For example, if α_i is zero-valued at all but one branch, the output results from selection combining or threshold combining; if α_i is nonzero for more than one branch, the output results from maximal-ratio combining or equal-gain combining.

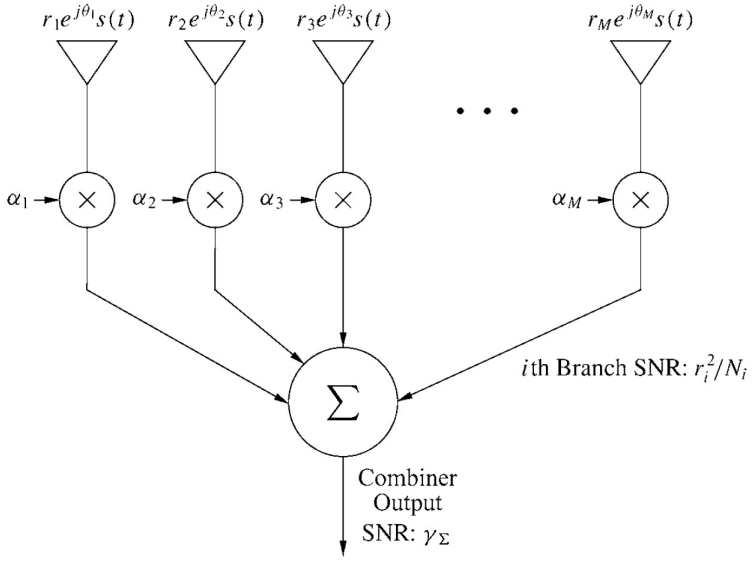

Figure 4.1: Linear combiner [6]

Selection combining (SC) is a combining technique where the the branch with the highest SNR is the one that is output, and the other $M-1$ branches are multiplied by $\alpha_i = 0$ and disregarded. For SC, the SNR gain increases with an increasing number of diversity branches but the relationship is not linear; the biggest gain occurs when

increasing from one branch to two [6]. If a system is continuously transmitting, the SNR at each branch will change so each branch requires its own receiver to monitor these changes. However, if threshold combining (TC) is used instead, only one receiver is needed to scan each branch. The receiver selects the first branch whose SNR is above a specified threshold and switches to scan another branch as soon as the SNR falls below the threshold.

To achieve better SNR gain, maximal-ratio combining (MRC) can be used to sum weighted versions of all the branches together. In order to allow coherent detection, the phase θ_i must be removed from the received signals through multiplication by $\alpha_i = a_i e^{-j\theta_i}$ where the gain of branch a_i is real. This is called co-phasing and is necessary when more than one branch is used in combining so that each signal has the same phase and there is no constructive or destructive interference. The resulting combiner SNR is equal to the sum of the SNRs on each branch. Thus, the array gain increases linearly with M [6]. Without knowing the SNR on each branch, MRC cannot be performed and instead equal gain combining (EGC) can be used to sum all of the branches together. For EGC, co-phasing is again necessary but $\alpha_i = e^{-j\theta_i}$ since $a_i = 1$ and each branch is equally weighted. Equal gain combining does not work as effectively as MRC since stronger signals are not weighted more heavily however the difference between EGC and MRC performance is typically less than 1 dB [6].

Chapter 5

Joint Spatial-Temporal Equalization

5.1 System Model

Building upon the previous work and theory discussed in the earlier chapters of this thesis, a joint spatial-temporal equalizer is developed to jointly optimize the combiner weights and equalizer coefficients for a multi-channel receiver. A synthetic ALE3G waveform is transmitted through a Watterson channel simulator and received using a uniform linear array (ULA). The signal received at each branch is then sampled every symbol prior to combining and equalizing.

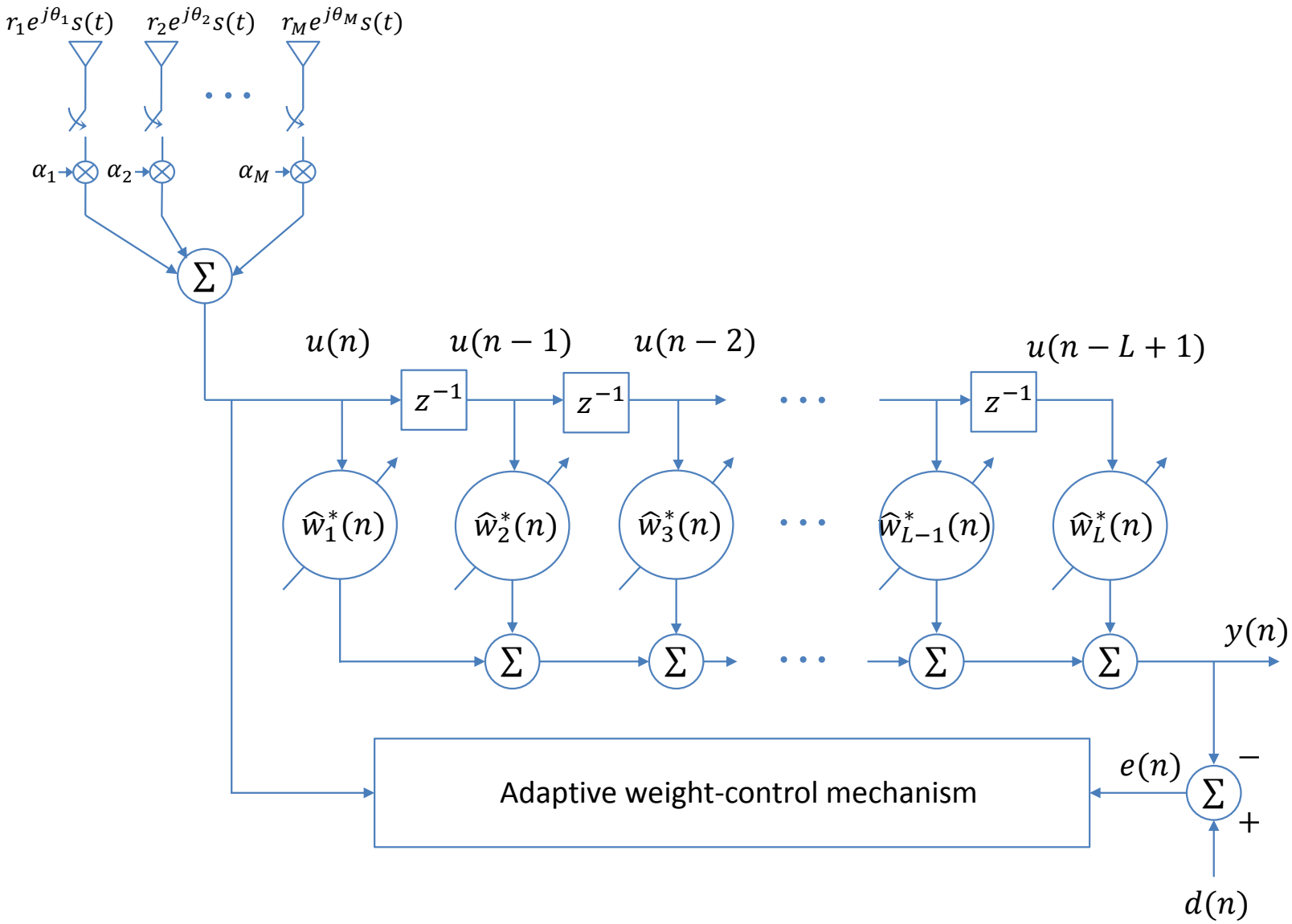

Figure 5.1: Linear combiner followed by single-channel equalizer

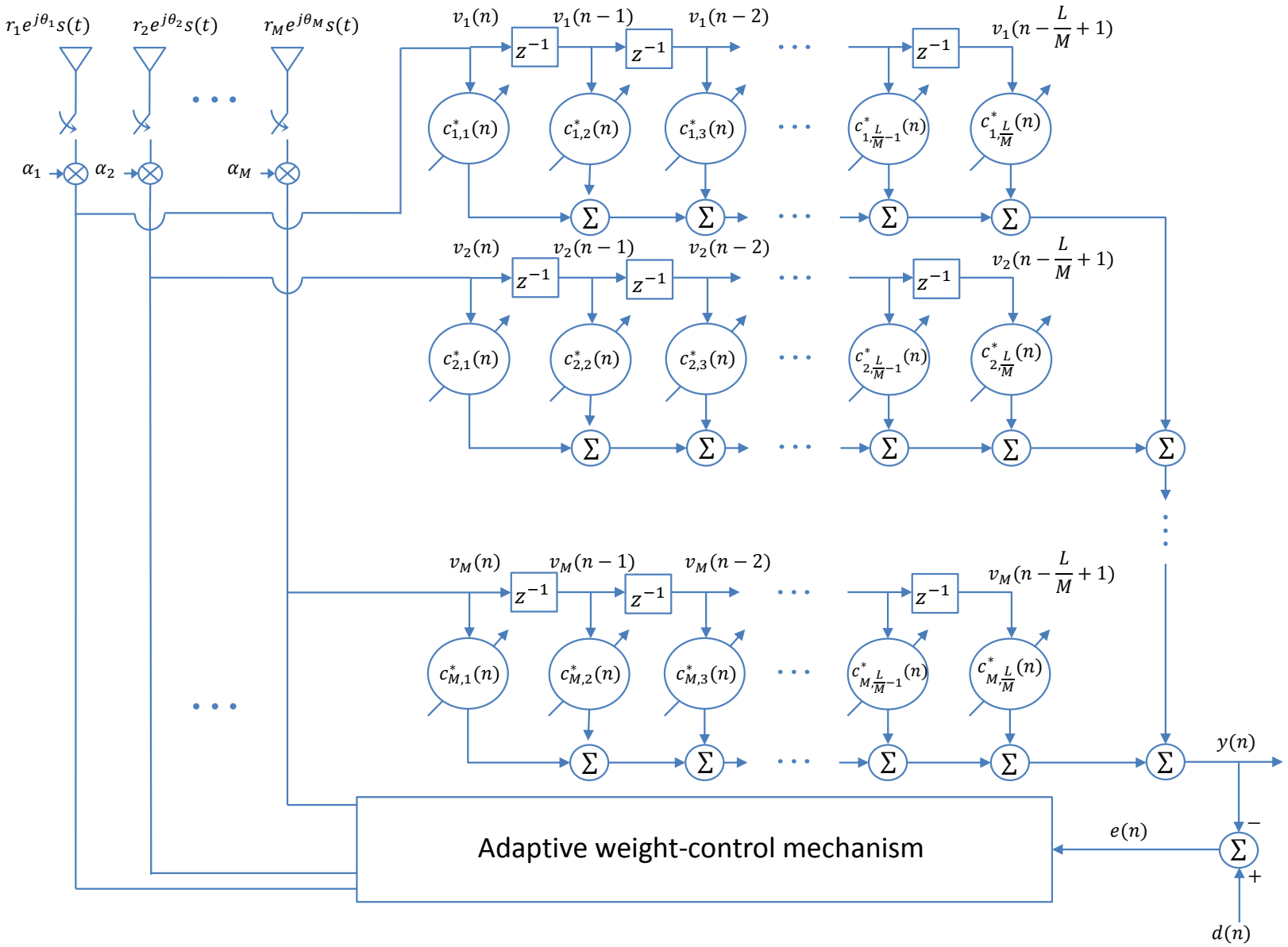

Figure 5.2: Joint spatial-temporal equalizer

Before deriving the joint spatial-temporal equalizer system model, it is important to understand the two-step system model of a linear combiner followed by equalization shown in Figure 5.1. The sampled received signal at the ith branch is given by $r_i e^{j\theta_i} s(n)$ where the only difference between this model and the linear combiner introduced in Chapter 4 is that the signals in this model are sampled every symbol. After being scaled by the combiner weights, the signal at the ith branch becomes $a_i r_i s(n)$ regardless of the combining method being MRC or EGC. After each of these signals are summed together, the combiner output is the input to a single-channel linear adaptive equalizer. The complex output of the equalizer $y(n)$ is demodulated and decoded as per the ALE3G standard as described in Chapter 2.

The joint spatial-temporal equalizer is different from the two-step system model previously discussed because it requires only one step to perform both temporal and spatial processing. The system model is shown in 5.2. For simplicity, we will only derive the LMS case, but the same derivation can be extended for the RLS case. The signals received at each antenna are passed through a tapped-delay line having L/M delay elements, where M is the total number of diversity branches and L is an integer:

$$\mathbf{v}_i(n) = [v_i(n), v_i(n-1), ..., v_i(n-L/M+1)] \tag{5.1}$$

and a composite input vector of length L is constructed:

$$\mathbf{u}(n) = [\mathbf{v}_1(n), \mathbf{v}_2(n), ..., \mathbf{v}_M(n)]^T \tag{5.2}$$

The combiner weights at each branch are given by

$$\hat{\mathbf{c}}_i(n) = [\hat{c}_{i,1}(n), \hat{c}_{i,2}(n), ..., \hat{c}_{i,L/M}(n)]^T \tag{5.3}$$

which are initialized to $\hat{\mathbf{c}}_i(n) = \mathbf{0}$ at the start of the algorithm. Each of these combiner weights are concatenated together to create a composite tap-weight vector of length L:

$$\hat{\mathbf{w}}^H(n) = [\hat{\mathbf{c}}_1^H(n), \hat{\mathbf{c}}_2^H(n), ..., \hat{\mathbf{c}}_M^H(n)] \tag{5.4}$$

and the filter output is given by

$$y(n) = \hat{\mathbf{w}}^H(n)\mathbf{u}(n) \tag{5.5}$$

The error signal $e(n)$ and estimated tap-weight vector update $\hat{\mathbf{w}}(n+1)$ are given in Chapter 3 (Equations 3.5 and 3.6) and reproduced here for convenience:

$$e(n) = d(n) - y(n)$$

$$\hat{\mathbf{w}}(n+1) = \hat{\mathbf{w}}(n) + \mu\mathbf{u}(n)e^*(n)$$

Note that there is a restriction on the selection of filter length L given M diversity branches; L must be a multiple of M. This constraint exists for ease of implementation and so that the same amount of spatial information from each branch is weighted and equalized. After symbol decisions are made, the waveform is demodulated and decoded.

5.2 Simulation Details

An ALE3G BW5 payload of 50 bits is formed into PSK symbols as described in Chapter 2. The symbols are then upsampled by an upsampling factor of four samples per symbol and filtered by a raised cosine pulseshaping filter with a stopband attenuation of 60 dB and a rolloff factor of 0.5. The modulated symbols are then

transmitted at 9600 symbols per second (the baud rate upsampled by four) through the ionosphere simulated using the Watterson model with mid-latitude quiet conditions: two paths, 0.1 Hz Doppler spread, 0.5 ms relative path delay, path gains of 0 dB and -1 dB, various SNR values ranging from -20 dB to 35 dB, and specified angles of arrival for each signal path.

A simulated array manifold is created for a ULA having between one and four isotropic elements spaced one half-wavelength apart. After the signal is received by the antenna array, it is downsampled and aligned in time according to its baud rate. For both the combiner followed by single-channel equalizer and joint spatial-temporal equalizer cases, the same equalizer parameters are used to give valid comparisons. Tap weights are initialized to all zeros, the total number of taps varies across simulations and ranges from 12 to 48, the step size (LMS) varies from 0.01 to 0.40, the regularization parameter (RLS) is 0.01, the forgetting factor (RLS) ranges from 0.85 to 0.99. After equalization, the symbols are demodulated and decoded according to the ALE3G BW5 standard and results are compared, evaluated, and discussed.

Chapter 6

Experimental Results

6.1 Introduction

The joint spatial-temporal equalizer was compared against two other diversity receiver structures: an EGC followed by a single-channel (temporal) equalizer, and an MRC followed by a single-channel equalizer. It is found that EGC and MRC performance are comparable for the simulations performed so for ease of legibility, the results presented in the following sections compare the joint spatial-temporal equalizer to only one other receiver structure. The next two sections present results for equalizer convergence and overall system performance through demodulation and decoding.

6.2 Equalizer Convergence

The joint spatial-temporal equalizer was compared against the single-channel equalizer following a linear combiner. For various SNRs, total number of tap weights, and step size μ (for LMS) or forgetting factor λ (for RLS), the convergence times and MSEs (where the error is the Euclidean distance between constellation points) were

recorded for four branches of diversity after averaging 20 independent trials and are shown in Table 6.1 and Table 6.2 where SCE refers to the single-channel equalizer after combining using an EGC and JSTE refers to the joint spatial-temporal equalizer. Convergence times are in terms of number of training symbols (out of 832) and are calculated by choosing a threshold and selecting the last training symbol that remained under the threshold as the point of convergence. The MSE was recorded as the error at the last training symbol. If neither equalizer converged before the last training symbol, convergence was not recorded. These tables are presented to help the reader understand the effect of different parameters on equalization. It should be noted that for many combinations of parameters, the equalizers converged but only after training mode ended; the results from these experiments were not recorded except for the LMS cases when the joint spatial-temporal equalizer converged during training but the single-channel equalizer did not.

There are only three runs of the LMS convergence simulations shown in Table 6.1 where the MSE for SCE is lower then the MSE for JSTE and not a single case where the SCE converged faster than the STE. There are also only three runs from Table 6.2 where the MSE was lower for SCE than JSTE and again no cases of faster convergence. For both the RLS and LMS algorithms, the joint spatial-temporal equalizer learns its tap weights faster than the single-channel equalizer and in general more closely approaches the optimal weights. This is an advantage especially for when there are short training sequences without any probes such as those seen in ALE3G BW0, BW1, BW3, and BW5.

For selected experiments, learning curves for 20 iterations and 8-PSK constellations for a single iteration are presented to offer side-by-side comparisons between the joint spatial-temporal equalizer and the combiner followed by single-channel equalizer. The

Table 6.1: Equalizer convergence comparisons, LMS

μ	Taps	SNR (dB)	Conv., SCE	Conv., JSTE	MSE, SCE	MSE, JSTE
0.05	24	10	–	570	0.0185	0.0017
0.05	24	20	–	270	0.0550	0.0009
0.05	24	35	–	733	0.0298	0.0004
0.05	36	10	–	553	0.0262	0.0050
0.05	36	20	–	727	0.0507	0.0003
0.10	12	10	–	130	0.0103	0.0059
0.10	12	20	–	339	0.0295	0.0101
0.10	24	10	–	266	0.0242	0.0138
0.10	24	20	–	225	0.0189	0.0009
0.10	36	10	–	714	0.0044	0.0162
0.10	36	20	–	523	0.0264	0.0002
0.10	48	10	–	254	0.0272	0.0071
0.10	48	20	–	400	0.0121	0.0003
0.15	12	10	–	551	0.0316	0.0081
0.15	12	20	–	784	0.0240	0.0018
0.15	24	10	–	95	0.0234	0.0089
0.15	24	20	774	335	0.0028	0.0004
0.15	36	10	–	417	0.0123	0.0114
0.15	36	20	–	546	0.0174	0.0018
0.20	12	10	–	227	0.0037	0.0065
0.20	12	20	389	296	0.0030	0.0004
0.20	24	20	719	136	0.0054	0.0008
0.20	36	10	–	127	0.0374	0.0052
0.20	36	20	792	274	0.0187	0.0317
0.30	12	10	–	73	0.0072	0.0063
0.30	12	20	749	616	0.0100	0.0004
0.40	12	10	144	58	0.0387	0.0101
0.40	12	20	351	205	0.0160	0.0008

learning curves are a way to visualize much of the same data presented in Table 6.1 and Table 6.2 and the symbol constellations show further affirmation that the equalizer is doing a good job at making symbol decisions. The symbol constellations tend to be more closely clustered around correct symbols for the joint spatial-temporal equalizer symbols. It should be noted that the constellations show all of the symbols in a

Table 6.2: Equalizer convergence comparisons, RLS

λ	Taps	SNR (dB)	Conv., SCE	Conv., JSTE	MSE, SCE	MSE, JSTE
0.99	12	20	502	476	0.0087	0.0002
0.99	24	10	559	379	0.0316	0.0062
0.99	24	20	600	446	0.0173	0.0007
0.99	36	10	556	376	0.0139	0.0028
0.99	36	20	693	586	0.0073	0.0094
0.99	48	10	589	430	0.0325	0.0036
0.99	48	20	693	587	0.0013	0.0012
0.95	12	10	275	110	0.0258	0.0076
0.95	12	20	791	679	0.0108	0.0010
0.95	24	10	123	76	0.0116	0.0182
0.95	24	20	143	137	0.0278	0.0020
0.95	36	10	123	76	0.0116	0.0182
0.95	36	20	143	137	0.0278	0.0020
0.95	48	20	208	123	0.0045	0.0009
0.90	12	10	58	54	0.0256	0.0017
0.90	12	20	69	69	0.0272	0.0009
0.90	24	10	69	51	0.0489	0.0061
0.90	24	20	79	74	0.0193	0.0037
0.90	36	10	86	51	0.0558	0.0267
0.90	36	20	81	67	0.0067	0.0012
0.90	48	10	109	51	0.0515	0.0295
0.90	48	20	96	62	0.0074	0.0049
0.85	12	10	70	33	0.0376	0.0124
0.85	12	20	54	46	0.0810	0.0014
0.85	24	10	54	37	0.0692	0.0260
0.85	24	20	192	43	0.0157	0.0052
0.85	24	30	58	50	0.0227	0.0002
0.85	36	20	66	49	0.0109	0.0024
0.85	48	20	87	47	0.0205	0.0148
0.85	48	30	96	53	0.0004	0.0003

transmission including the transient period before the equalizers converged.

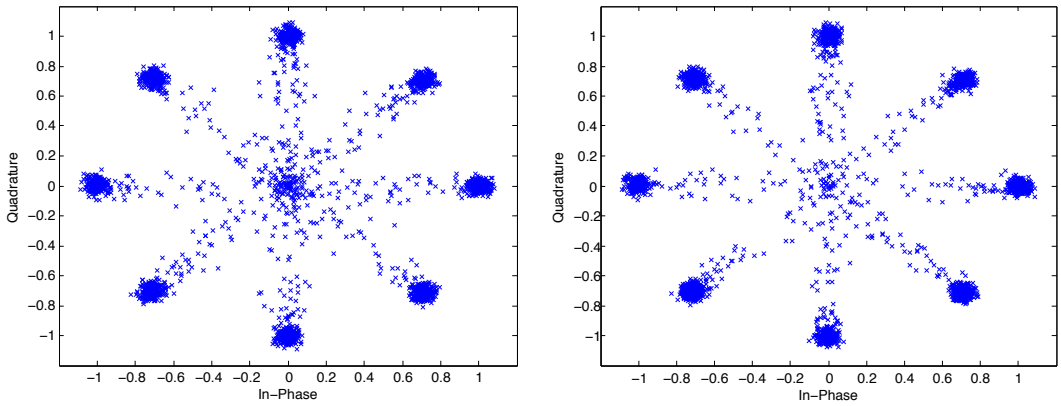

(a) EGC + single-channel equalizer (b) Joint spatial-temporal equalizer

Figure 6.1: Equalized symbols: 24 taps, RLS(0.99), SNR 20 dB, 4 diversity branches

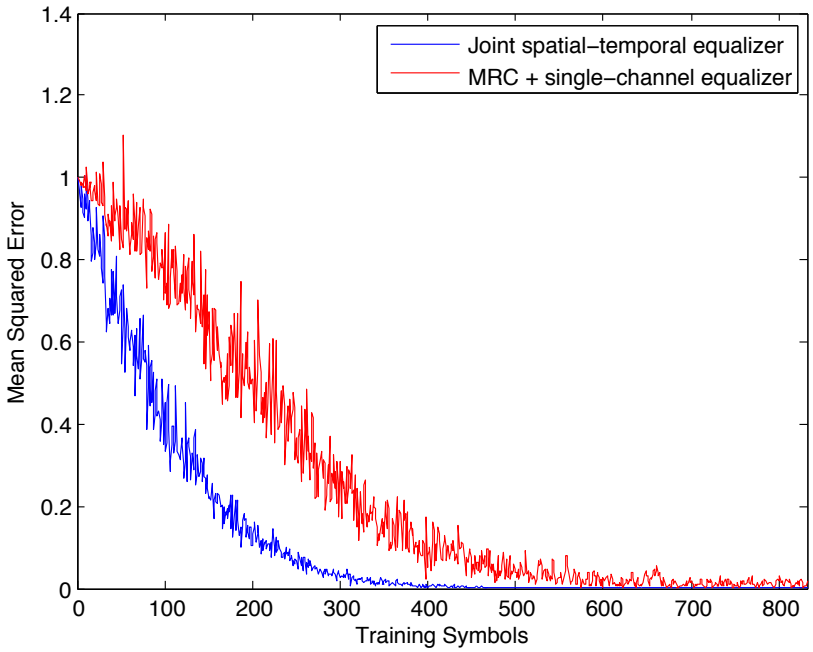

Figure 6.2: Learning curves: 24 taps, RLS(0.99), SNR 20 dB, 4 diversity branches

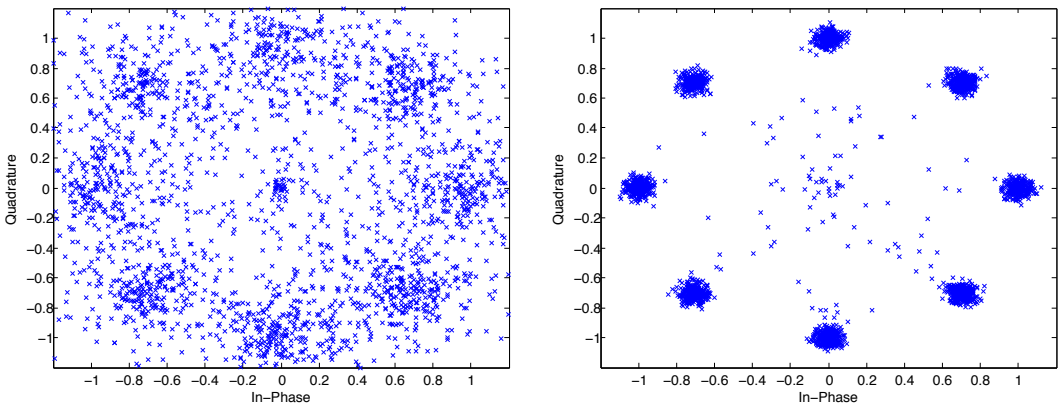

(a) EGC + single-channel equalizer (b) Joint spatial-temporal equalizer

Figure 6.3: Equalized symbols: 24 taps, RLS(0.95), SNR 20 dB, 4 diversity branches

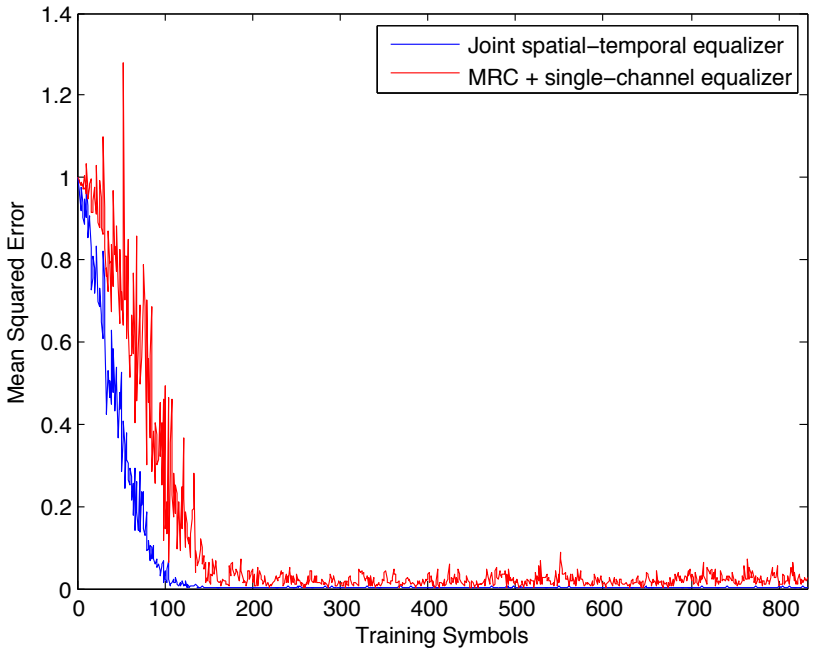

Figure 6.4: Learning curves: 24 taps, RLS(0.95), SNR 20 dB, 4 diversity branches

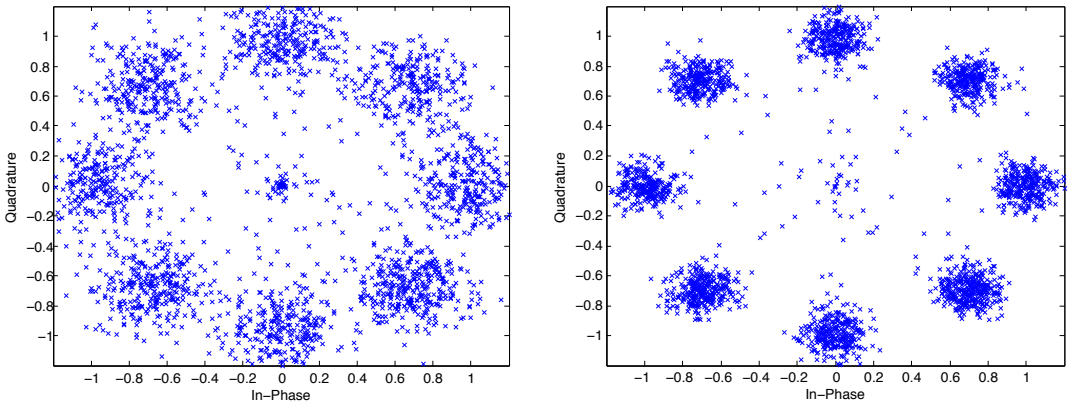

(a) EGC + single-channel equalizer (b) Joint spatial-temporal equalizer

Figure 6.5: Equalized symbols: 12 taps, RLS(0.95), SNR 10 dB, 4 diversity branches

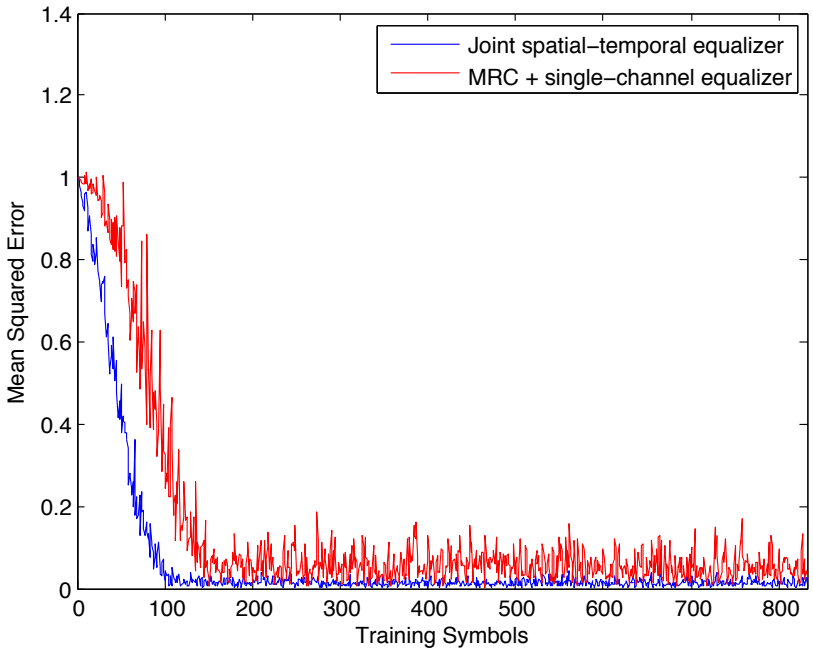

Figure 6.6: Learning curves: 12 taps, RLS(0.95), SNR 10 dB, 4 diversity branches

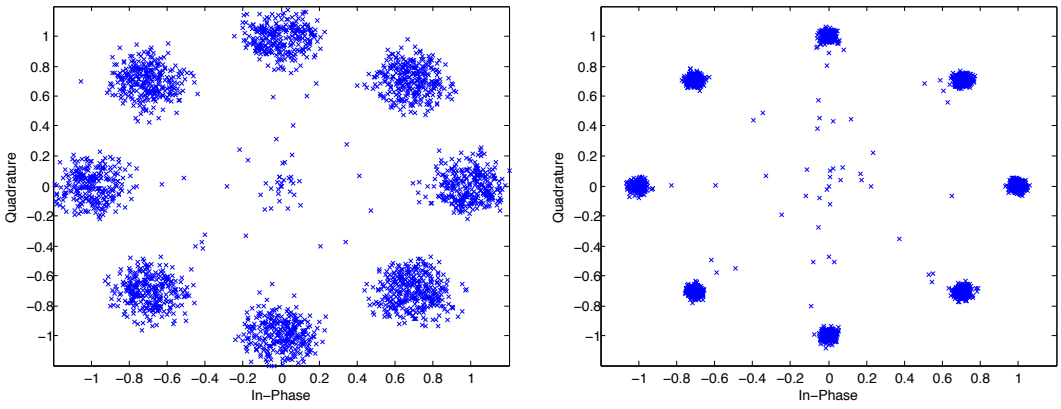

(a) EGC + single-channel equalizer (b) Joint spatial-temporal equalizer

Figure 6.7: Equalized symbols: 12 taps, RLS(0.90), SNR 20 dB, 4 diversity branches

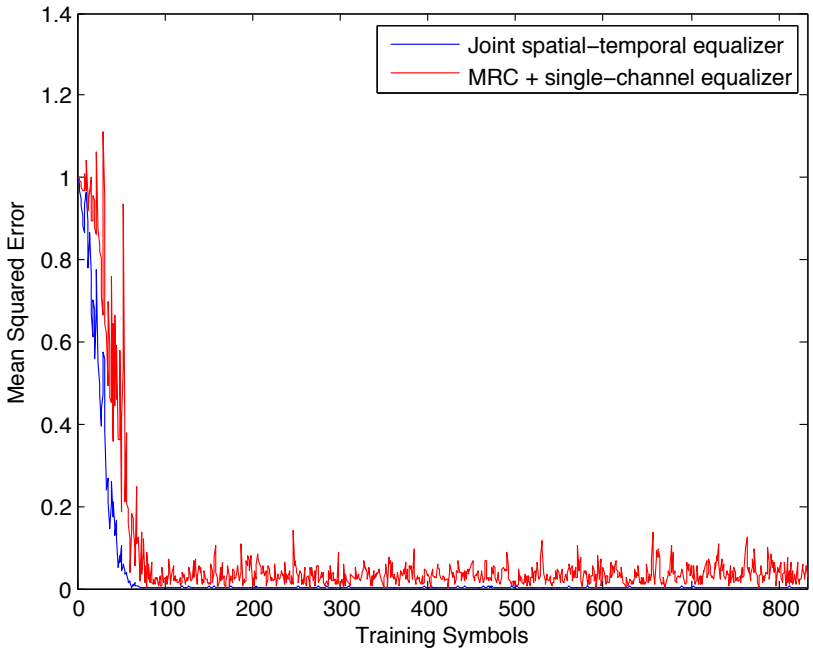

Figure 6.8: Learning curves: 12 taps, RLS(0.90), SNR 20 dB, 4 diversity branches

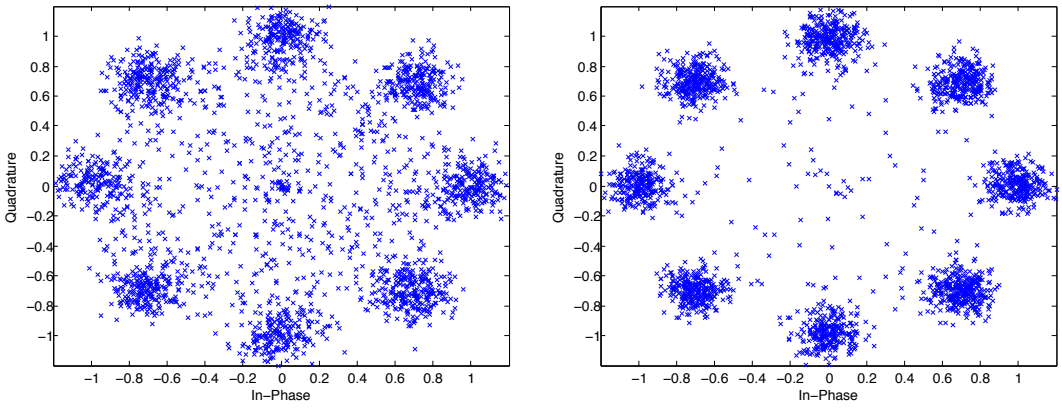

(a) EGC + single-channel equalizer (b) Joint spatial-temporal equalizer

Figure 6.9: Equalized symbols: 36 taps, LMS(0.05), SNR 10 dB, 4 diversity branches

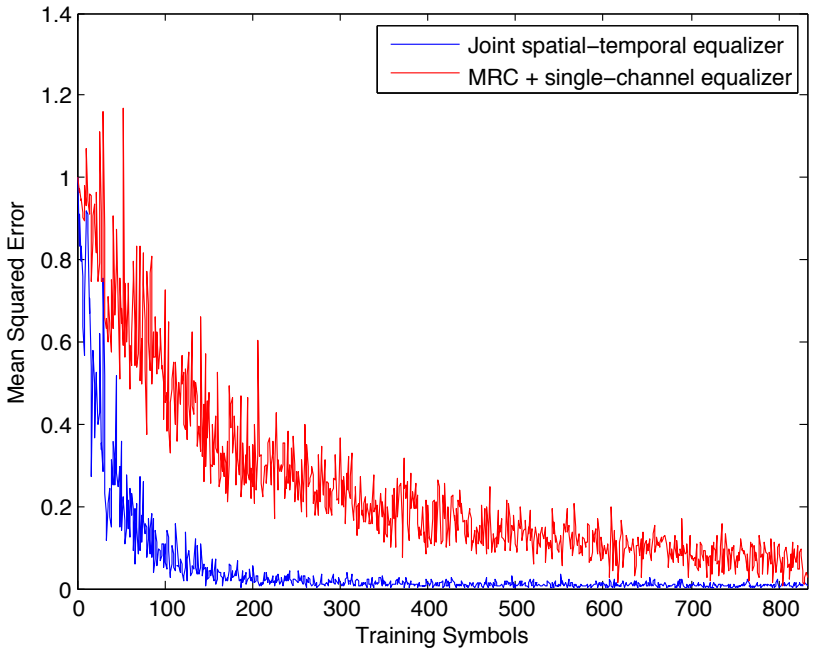

Figure 6.10: Learning curves: 36 taps, LMS(0.05), SNR 10 dB, 4 diversity branches

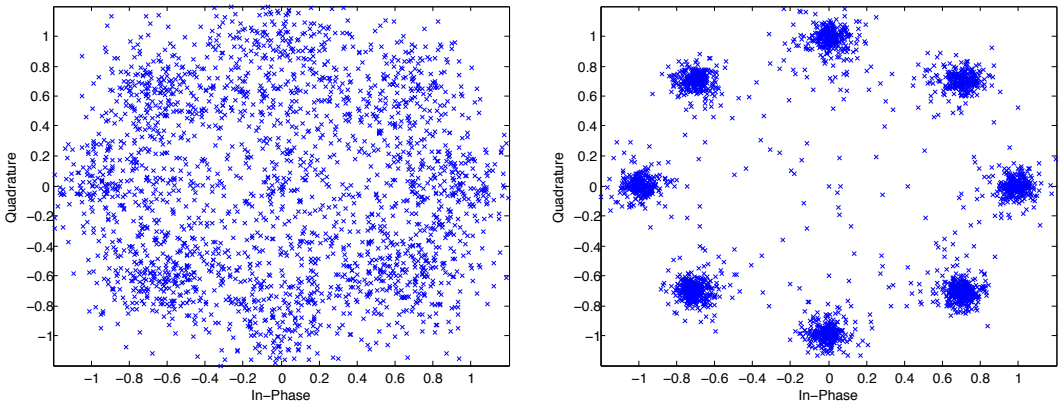

(a) EGC + single-channel equalizer (b) Joint spatial-temporal equalizer

Figure 6.11: Equalized symbols: 36 taps, LMS(0.10), SNR 20 dB, 4 diversity branches

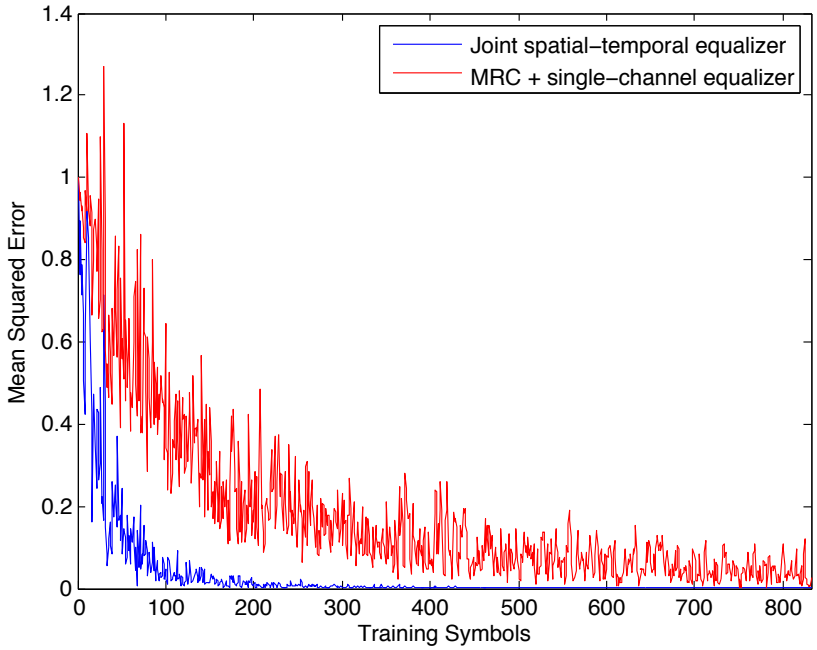

Figure 6.12: Learning curves: 36 taps, LMS(0.10), SNR 20 dB, 4 diversity branches

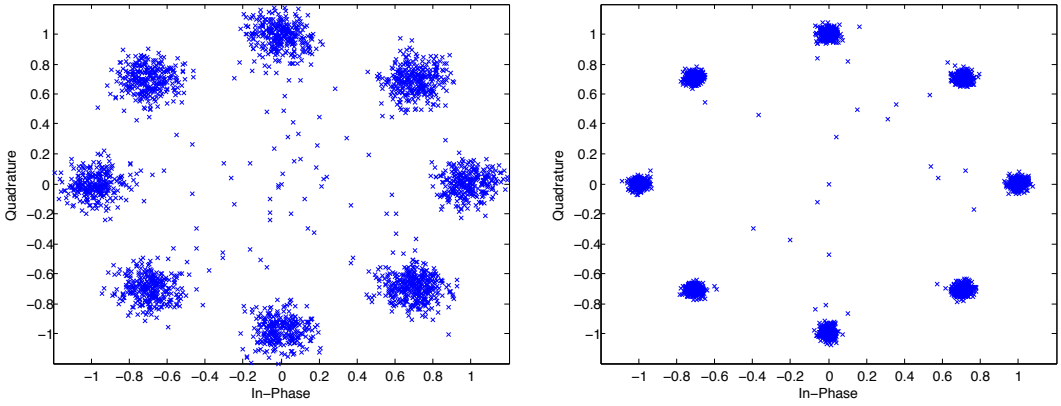

(a) EGC + single-channel equalizer (b) Joint spatial-temporal equalizer

Figure 6.13: Equalized symbols: 12 taps, LMS(0.15), SNR 20 dB, 4 diversity branches

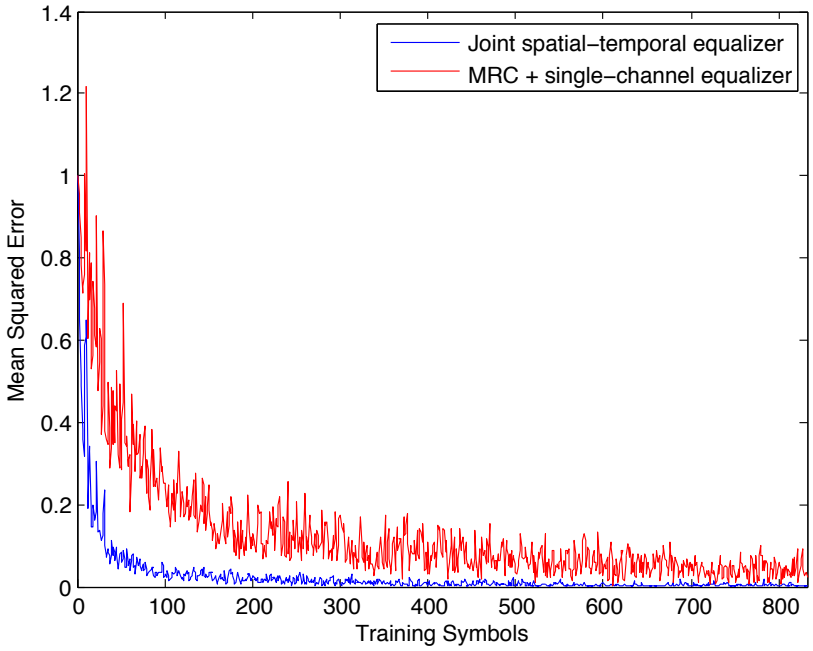

Figure 6.14: Learning curves: 12 taps, LMS(0.15), SNR 20 dB, 4 diversity branches

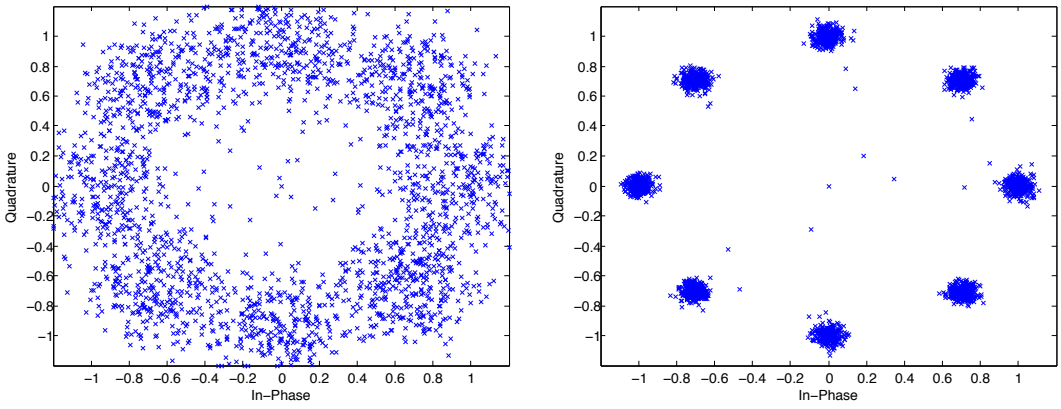

(a) EGC + single-channel equalizer (b) Joint spatial-temporal equalizer

Figure 6.15: Equalized symbols: 12 taps, LMS(0.40), SNR 20 dB, 4 diversity branches

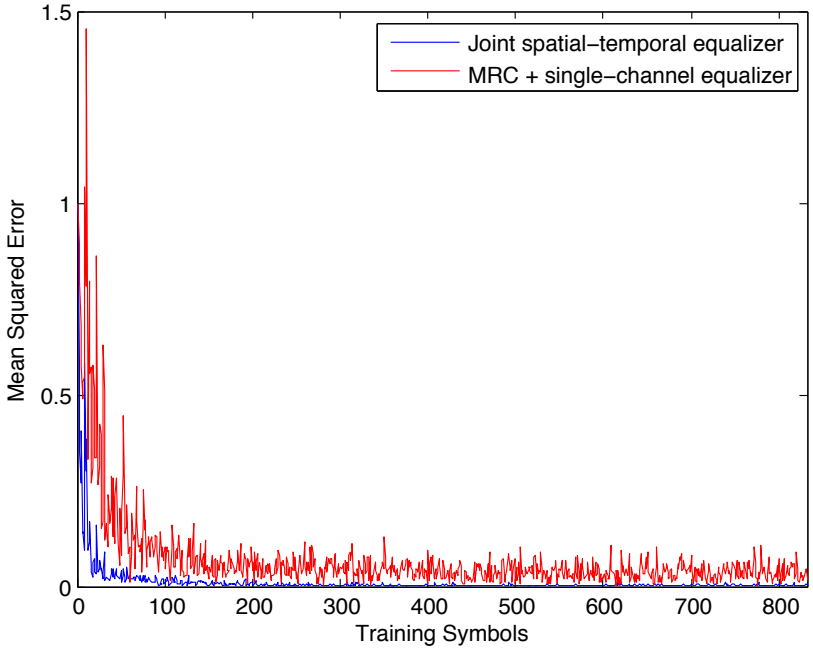

Figure 6.16: Learning curves: 12 taps, LMS(0.40), SNR 20 dB, 4 diversity branches

6.3 Receiver Performance

In order to measure how well the entire systems are performing through demodulation and decoding, bit error rates (BERs) are plotted against various signal-to-noise ratios (SNRs) for all three diversity receivers. Each simulation is averaged over 1000 independent trials and the results are presented in Figures 6.17, 6.18, 6.19, 6.20.

Figure 6.17 shows the BER for SNRs of -20 dB to 5 dB for two 12-tap RLS equalizers with forgetting factors of 0.99. This combination of parameters performs the best overall for all three receivers at low SNRs, but the EGC receiver is left out of the plot for clarity since it performs similarly to MRC; this is also the case for subsequent simulations. With increasing the number of equalizer filter taps but holding other parameters the same, performance across all receivers drops slightly because there are more weights to be learned. The joint spatial-temporal equalizer has less than 1 dB improvement for two branches of diversity, 1.5 dB improvement for three branches, and 2 dB improvement for four branches.

Figure 6.18 shows the BER for SNRs of -10 dB to 20 dB for two 12-tap RLS equalizers with forgetting factors of 0.95. Decreasing the forgetting factor from 0.99 results in good performance but for a higher range of SNRs. This figure more clearly shows the performance gain of the joint spatial-temporal equalizer; there is a 6 dB improvement for two branches of diversity, 9 dB improvement for three branches, and 10 dB improvement for four branches. Reducing the forgetting factor to 0.90 as shown in Figure 6.19 illustrates an even greater performance gap between the joint spatial-temporal equalizer and the MRC followed by single-channel equalizer. However, overall performance drops slightly for the JSTE and drastically for the other receivers. The majority of the LMS simulations did not work as well as the RLS equalizers. As seen in Figure 6.20, the MRC receiver performs better than JSTE at the

lowest SNRs. At -8.5 dB, the JSTE for two diversity branches begins to outperform but not significantly. For three diversity branches, the JSTE begins to perform better than MRC at around -10 dB and shows a 1 dB improvement. At -11 dB, the JSTE for four diversity branches begins to outperform and reaches an improvement of 2 dB.

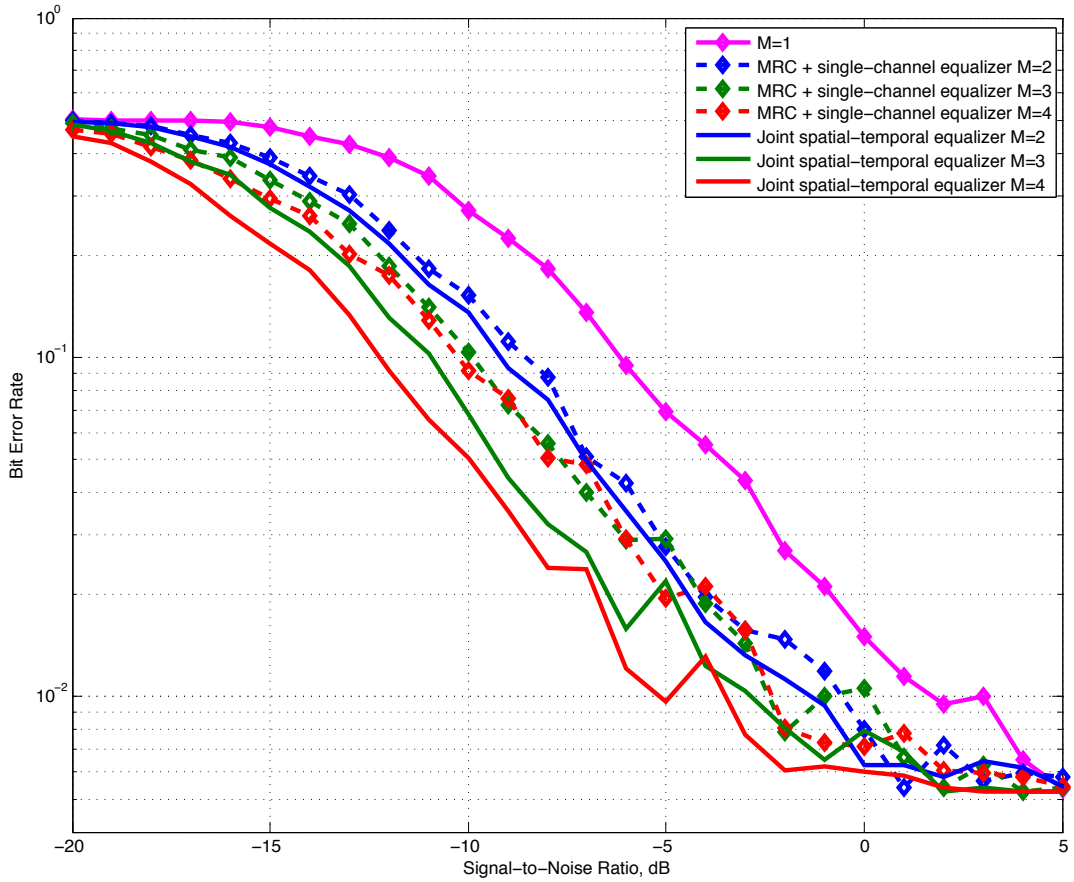

Figure 6.17: BER versus SNR for two receivers: 12 taps, RLS(0.99)

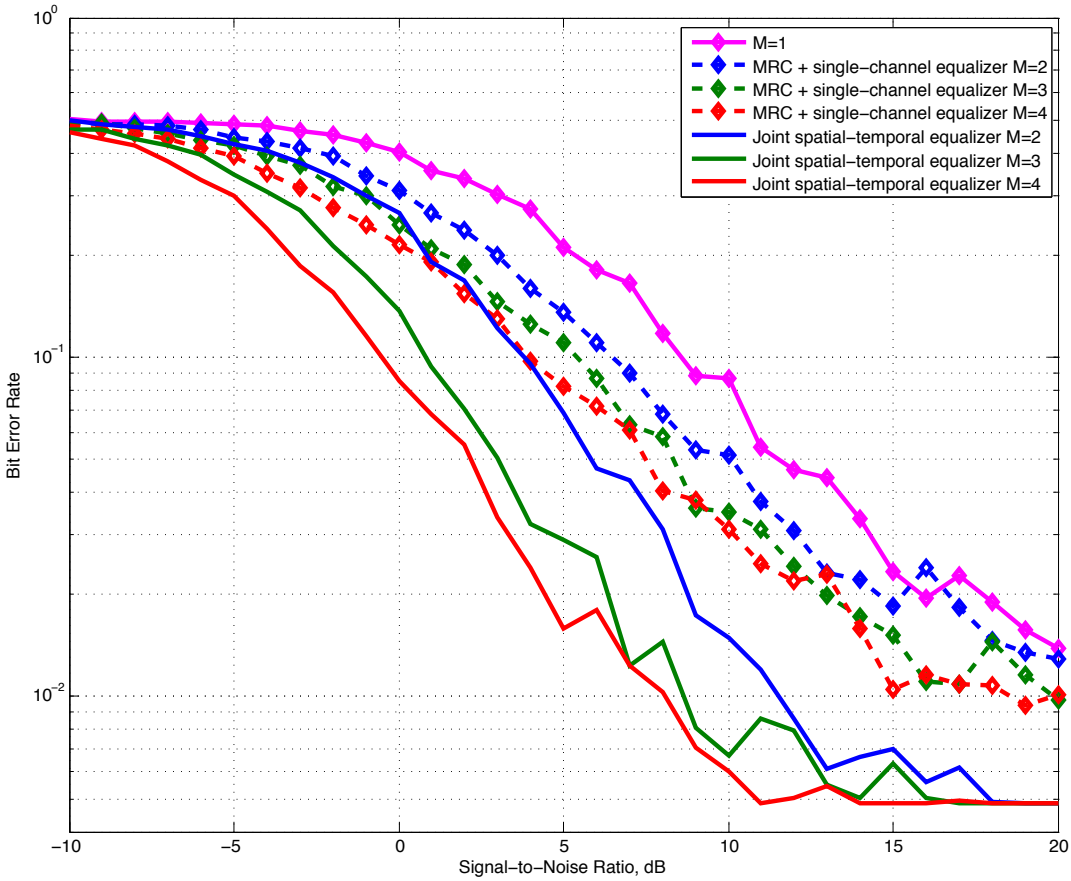

Figure 6.18: BER versus SNR for two receivers: 12 taps, RLS(0.95)

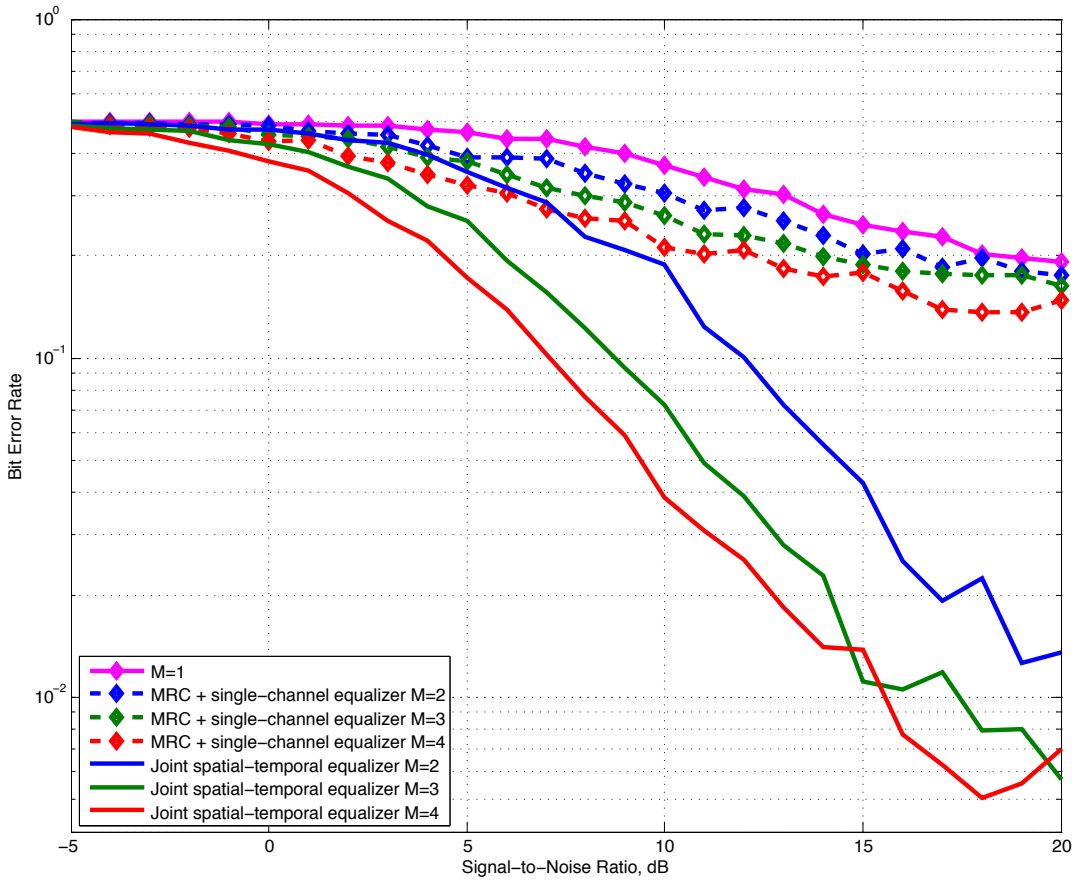

Figure 6.19: BER versus SNR for two receivers: 12 taps, RLS(0.90)

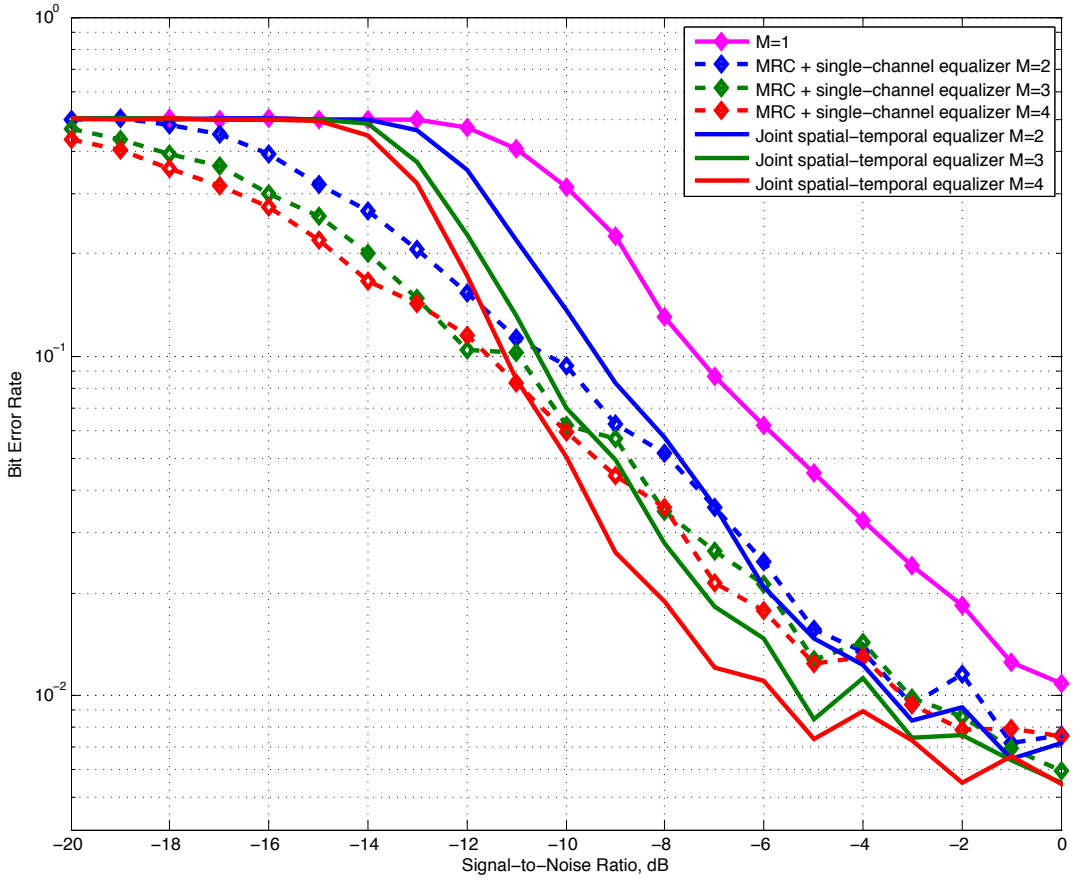

Figure 6.20: BER versus SNR for two receivers: 24 taps, LMS(0.01)

Chapter 7

Conclusions and Future Work

The joint spatial-temporal equalizer outperformed linear combiners followed by single-channel equalization under many different conditions in terms of equalizer convergence times, equalizer MSE, and overall BER, especially at low SNRs. By jointly combining and equalizing, there is no need to compute the channel gain or perform co-phasing of received signals. For an SDR framework that uses a dataflow architecture, this is advantageous since the receiver requires less software components to perform combining and equalizing. The proposed algorithm is easily scalable for multiple input channels if a software defined receiver already implements a single-channel equalizer.

Possible avenues for future work include implementing and testing different adaptive algorithms for linear equalizer tap-weight estimation, using fractionally spaced equalization instead of symbol-spaced, or using a nonlinear equalizer such as a DFE. Another avenue to explore for future work is to treat the equalizer as a classifier and use machine learning algorithms to learn the combiner and equalizer weights for a spatial-temporal equalizer. Lastly, rewriting the code in python and C++ and testing the algorithm with live multi-channel data on a Southwest Research Institute system

is another potential opportunity for future work.

Appendix A

MATLAB Code

The following MATLAB functions were used for the simulations in this thesis. The script `ALE3G_Watterson_EqCompare` calls the functions `ALE3Gmod`, `ALE3Gdemod`, `equalizer`, and `ChannelSimulator_v5`, an HF channel simulator modified from one originally written by Ryan Casey of Southwest Research Institute.

A.1 ALE3G Signal Generator

```
function [msg,tx,upsamp,syms] = ALE3Gmod(BW)
% ALE3G modulation
% 8-PSK, 1800 Hz carrier, 2400 baud

% parameters
%Fc = 1800;         % carrier frequency, Hz
%baud = 2400;       % symbols per second
upsamp = 4;        % upsample factor, samples per symbol
%Fs = upsamp*baud; % sampling frequency, Hz

% TLC/AGC guard sequence, 256 syms
tlc = textread('tlcagc.txt','%n');

switch BW
```

```
15      case '0'
16          bits = 26;                  % number of payload bits
17          constlen = 7;               % encoder constraint length
18          codegen = [133 171];        % generator polynomials in octal
19          row = 4; col = 13;          % interleaving matrix
20          base = 16;                  % for mapping bits to syms
21          chip = 64;
22          pn = 'PNseqBW0.txt';        % pn scrambling sequence
23          pre = 'pre0.txt';           % preamble
24          payload = 832;              % number of payload syms
25      case '1'
26          bits = 48;
27          constlen = 9;
28          codegen = [711 663 557];
29          row = 16; col = 9;
30          base = 16;
31          chip = 64;
32          pn = 'PNseqBW1.txt';
33          pre = 'pre1.txt';
34          payload = 2304;
35      case '1+'
36          bits = 51;
37          constlen = 7;
38          codegen = [133 171];
39          puncpat = [1,1,0];
40          base = 16;
41          chip = 32;
42          pn = 'PNseqBW1.txt';
43          tlc = tlc(1:192);
44          pre = 'pre1plus.txt';
45          payload = 544;
46      case '2' % make add'l cases for variable lengths
47          constlen = 8;
48          codegen = [];
49          pn = 'PNseqBW2.txt';
50          tlc = tlc(1:240);
51          pre = 'pre2.txt';
52          %payload = 2880; %5760,11520,23040, 304+(n*960), n=3,6,12,24
53      case '3' % make add'l cases for variable lengths
54          constlen = 7;
55          codegen = [];
56          base = 16;
57          chip = 16;
```

```
58          pn = 'PNseqBW3.txt';
59          tlc = 0;
60          pre = 'pre3.txt';
61          %payload = 2304; %4352,8448,16640
62      case '4'
63          bits = 2;
64          base = 4;
65          chip = 1280;
66          pn = 'PNseqBW4.txt';
67          payload = 1280;
68      case '5'
69          %crc = []; % 8-bit CRC
70          bits = 50;
71          constlen = 7;
72          codegen = [133 171];
73          row = 10; col = 10;
74          base = 16;
75          chip = 64;
76          pn = 'PNseqBW5.txt';
77          pre = 'pre5.txt';
78          payload = 1600;
79  end
80
81  % binary data stream
82  msg = round(rand(bits,1));
83  % crc = CRC_BW5(msg,poly,etc.)
84  %msg = cat(1,msg,crc);
85
86  if ~strcmp(BW,'4')
87      % FEC
88      init_state = msg(end:-1:bits-constlen+2); % last constlen-1 bits
89      init_state = bin2dec(num2str(init_state'));
90      trellis = poly2trellis(constlen,codegen);
91      if ~strcmp(BW,'1+')
92          coded = convenc(msg,trellis,init_state);
93      else
94          coded = convenc(msg,trellis,puncpat,init_state);
95      end
96      % CHECK: viterbi decode
97      % tblen = 5*constlen;
98      % vit = vitdec([coded;coded],trellis,tblen,'trunc','hard');
99      % vit = vit(bits+1:end); % check: is vit same as msg?
100     % sum(vit == msg) % should = 50 for BW5
```

```
101
102     if ~strcmp(BW,'1+')
103         % interleave
104         deintrlvd = reshape(coded,row,col);
105         intrlvd = reshape(deintrlvd',row*col,1);
106         % CHECK: deinterleave
107         % i = reshape(intrlvd,col,row)';
108         % codedBits = reshape(i,col*row,1);
109         % sum(codedBits == coded) % should = 100 for BW5
110
111         % base change
112         bc = reshape(intrlvd,log2(base),row*col/log2(base))';
113     else % BW 1+ - yes FEC but no interleaving
114         bc = reshape(coded,log2(base),length(coded)/log2(base))';
115     end
116 else % BW 4 - no FEC or interleaving
117     bc = reshape(msg,log2(base),bits/log2(base))';
118 end
119 corr = bin2dec(num2str(bc));
120
121 % walsh modulation
122 if strcmp(BW,'4')
123     % Table C-XVIII, mapped to complex [0,4] --> [1,-1]
124     tribitSeq       = zeros(chip,4);
125     tribitSeq(:,1)  = ones(chip,1);                 % 00
126     tribitSeq(:,2)  = repmat([1;-1;1;-1],chip/4,1); % 01
127     tribitSeq(:,3)  = repmat([1;1;-1;-1],chip/4,1); % 10
128     tribitSeq(:,4)  = repmat([1;-1;-1;1],chip/4,1); % 11
129 else
130     % Table C-VIII, mapped to complex [0,4] --> [1,-1]
131     tribitSeq       = zeros(chip,16);
132     tribitSeq(:,1)  = ones(chip,1);                                     % 0000
133     tribitSeq(:,2)  = repmat([1;-1;1;-1],chip/4,1);                     % 0001
134     tribitSeq(:,3)  = repmat([1;1;-1;-1],chip/4,1);                     % 0010
135     tribitSeq(:,4)  = repmat([1;-1;-1;1],chip/4,1);                     % 0011
136     tribitSeq(:,5)  = repmat([1;1;1;1;-1;-1;-1;-1],chip/8,1);           % 0100
137     tribitSeq(:,6)  = repmat([1;-1;1;-1;-1;1;-1;1],chip/8,1);           % 0101
138     tribitSeq(:,7)  = repmat([1;1;-1;-1;-1;-1;1;1],chip/8,1);           % 0110
139     tribitSeq(:,8)  = repmat([1;-1;-1;1;-1;1;1;-1],chip/8,1);           % 0111
140     tribitSeq(:,9)  = repmat([ones(8,1);-1*ones(8,1)],chip/16,1);       % 1000
141     tribitSeq(:,10) = repmat([repmat([1;-1],4,1);repmat([-1;1],4,1)],...
142                                                         chip/16,1);     % 1001
143     tribitSeq(:,11) = repmat([1;1;-1;-1;1;1;-1;-1;-1;-1;1;1;-1;-1;1;1],...
```

```
144                                                         chip/16,1);  % 1010
145     tribitSeq(:,12) = repmat([1;-1;-1;1;1;-1;-1;1;-1;1;1;-1;-1;1;1;-1],...
146                                                         chip/16,1);  % 1011
147     tribitSeq(:,13) = repmat([ones(4,1);-1*ones(8,1);ones(4,1)],...
148                                                         chip/16,1);  % 1100
149     tribitSeq(:,14) = repmat([1;-1;1;-1;repmat([-1;1],4,1);1;-1;1;-1],...
150                                                         chip/16,1);  % 1101
151     tribitSeq(:,15) = repmat([1;1;-1;-1;-1;-1;1;1;-1;-1;1;1;1;1;-1;-1],...
152                                                         chip/16,1);  % 1110
153     tribitSeq(:,16) = repmat([1;-1;-1;1;-1;1;1;-1;1;1;-1;1;-1;-1;1;1],...
154                                                         chip/16,1);  % 1111
155 end
156
157 chunks = payload/chip;
158 correlated = corr + ones(chunks,1); % fix matlab indexing
159
160 y = zeros(chip,chunks);
161 for i = 1:chunks
162     y(:,i) = tribitSeq(:,correlated(i));
163 end
164 % CHECK: correlate
165 % y = y.';
166 % yy = y*tribitSeq; % inner product
167 % [maxVals, cor] = max(yy,[],2);
168 % sum(cor == correlated) % should = 25 for BW5
169 walsh = reshape(y,payload,1);
170
171 % PN spreading
172 PNseq = textread(pn,'%n');
173 PNseq_IQ = exp((-1j*2*pi/8)*PNseq); % map to complex conjugate
174 lenpn = length(PNseq);
175 reps = payload/lenpn;
176 PNseq_IQ = repmat(PNseq_IQ,ceil(reps),1);
177 PNseq_IQ = PNseq_IQ(1:payload);
178 PNsyms = walsh./PNseq_IQ;
179 % CHECK: descramble
180 % descrambled = PNseq_IQ.*syms; % component-wise mod 8 addition
181 % sum(descrambled == walsh); % should = 1600 for BW5
182
183 % add TLC/AGC + preamble
184 if strcmp(BW,'4')
185     preamble = [];
186 else
```

```
    preamble = textread(pre,'%n');
end
presyms = cat(1,tlc,preamble); % TLC/AGC + preamble tribit symbols

% map tribits to phases
presyms = exp(1j*2*pi/8*presyms);

% append TLC/AGC + preamble to beginning of payload symbols
syms = cat(1,presyms,PNsyms);
% figure()
% plot(syms,'o')
% axis([-1.2 1.2 -1.2 1.2])

% modulate onto carrier
upsyms = upsample(syms,upsamp);
h = fdesign.pulseshaping(upsamp,'Raised Cosine','Ast,Beta',60,0.50);
Hd = design(h);
filtered = conv(Hd.Numerator, upsyms);
del = (length(Hd.Numerator)-1)/2; % group delay
tx = filtered(del+1:end-del);
```

A.2 ALE3G Demodulator

```
function [bits] = ALE3Gdemod(BW,tx,graph)
% ALE3G demodulation

% parameters
switch BW
    case '0'
        tlc = 256;                  % number of tlc/agc syms
        preamble = 384;             % number of preamble syms
        payload = 832;              % number of payload syms
        filename = 'PNseqBW0.txt';  % pn descrambling sequence
        chip = 64;
        row = 4; col = 13;          % deinterleaving matrix
        rate = 1/2;                 % decoder rate
        constlen = 7;               % decoder constraint length
        codegen = [133 171];        % generator polynomials in octal
    case '1'
        tlc = 256;
        preamble = 576;
```

```
19          payload = 2304;
20          filename = 'PNseqBW1.txt';
21          chip = 64;
22          row = 16; col = 9;
23          rate = 1/3;
24          constlen = 9;
25          codegen = [711 663 557];
26      case '1+'
27          tlc = 192;
28          preamble = 192;
29          payload = 544;
30          filename = 'PNseqBW1.txt';
31          chip = 32;
32          rate = 3/4;
33          constlen = 7;
34          codegen = [133 171];
35          puncpat = [1,1,0];
36      case '2' % make add'l cases for variable lengths
37          tlc = 240;
38          preamble = 64;
39          %payload = 2880; %5760,11520,23040, 304+(n*960), n=3,6,12,24
40          filename = 'PNseqBW2.txt';
41          rate = 1/2;
42          constlen = 8;
43          codegen = [];
44      case '3' % make add'l cases for variable lengths
45          tlc = 0;
46          preamble = 640;
47          %payload = 2304; %4352,8448,16640
48          filename = 'PNseqBW3.txt';
49          chip = 16;
50          rate = 1/2;
51          constlen = 7;
52          codegen = [];
53      case '4'
54          tlc = 256;
55          preamble = 0;
56          payload = 1280;
57          filename = 'PNseqBW4.txt';
58          chip = 1280;
59      case '5'
60          tlc = 256;
61          preamble = 576;
```

```
        payload = 1600;
        filename = 'PNseqBW5.txt';
        chip = 64;
        row = 10; col = 10;
        rate = 1/2;
        constlen = 7;
        codegen = [133 171];
end

% we only want the payload syms - trim off preamble
trimmedSyms = tx(tlc+preamble+1:tlc+preamble+payload);

% descramble
PNseq = textread(filename,'%n');
lenpn = length(PNseq);
reps = payload/lenpn;
PNseq_IQ = exp((-1j*2*pi/8)*PNseq);
PNseq_IQ = repmat(PNseq_IQ,ceil(reps),1);
PNseq_IQ = PNseq_IQ(1:payload);

descrambled = PNseq_IQ.*trimmedSyms; % component-wise mod 8 addition
if graph==1
    figure()
    plot(descrambled,'o') % 8-PSK becomes BPSK
    axis([-1.2 1.2 -1.2 1.2])
    title('Descrambled Syms')
end

% symbol error rate
%d = csvread('descrambled.txt');
%descrambled_exp = d(:,1) + 1j*d(:,2);
%symerr = 100*numel(find(abs(descrambled_exp - descrambled)>0.01))/payload;

% normalize to unit vectors to get rid of outliers
normalized = zeros(length(descrambled),1);
for i = 1:length(descrambled)
    normalized(i) = descrambled(i)/norm(descrambled(i));
end

% correlate
if strcmp(BW,'4')
    % Table C-XVIII, mapped to complex [0,4] --> [1,-1]
    tribitSeq       = zeros(chip,4);
```

```
105     tribitSeq(:,1)  = ones(chip,1);                % 00
106     tribitSeq(:,2)  = repmat([1;-1;1;-1],chip/4,1); % 01
107     tribitSeq(:,3)  = repmat([1;1;-1;-1],chip/4,1); % 10
108     tribitSeq(:,4)  = repmat([1;-1;-1;1],chip/4,1); % 11
109 else
110     % Table C-VIII, mapped to complex [0,4] --> [1,-1]
111     tribitSeq       = zeros(chip,16);
112     tribitSeq(:,1)  = ones(chip,1);                                     % 0000
113     tribitSeq(:,2)  = repmat([1;-1;1;-1],chip/4,1);                     % 0001
114     tribitSeq(:,3)  = repmat([1;1;-1;-1],chip/4,1);                     % 0010
115     tribitSeq(:,4)  = repmat([1;-1;-1;1],chip/4,1);                     % 0011
116     tribitSeq(:,5)  = repmat([1;1;1;1;-1;-1;-1;-1],chip/8,1);           % 0100
117     tribitSeq(:,6)  = repmat([1;-1;1;-1;-1;1;-1;1],chip/8,1);           % 0101
118     tribitSeq(:,7)  = repmat([1;1;-1;-1;-1;-1;1;1],chip/8,1);           % 0110
119     tribitSeq(:,8)  = repmat([1;-1;-1;1;-1;1;1;-1],chip/8,1);           % 0111
120     tribitSeq(:,9)  = repmat([ones(8,1);-1*ones(8,1)],chip/16,1);       % 1000
121     tribitSeq(:,10) = repmat([repmat([1;-1],4,1);repmat([-1;1],4,1)],...
122                                                         chip/16,1);     % 1001
123     tribitSeq(:,11) = repmat([1;1;-1;-1;1;1;-1;-1;-1;-1;1;1;-1;-1;1;1],...
124                                                         chip/16,1);     % 1010
125     tribitSeq(:,12) = repmat([1;-1;-1;1;1;-1;-1;1;-1;1;1;-1;-1;1;1;-1],...
126                                                         chip/16,1);     % 1011
127     tribitSeq(:,13) = repmat([ones(4,1);-1*ones(8,1);ones(4,1)],...
128                                                         chip/16,1);     % 1100
129     tribitSeq(:,14) = repmat([1;-1;1;-1;repmat([-1;1],4,1);1;-1;1;-1],...
130                                                         chip/16,1);     % 1101
131     tribitSeq(:,15) = repmat([1;1;-1;-1;-1;-1;1;1;-1;-1;1;1;1;1;-1;-1],...
132                                                         chip/16,1);     % 1110
133     tribitSeq(:,16) = repmat([1;-1;-1;1;-1;1;1;-1;1;1;-1;1;-1;-1;1;1],...
134                                                         chip/16,1);     % 1111
135 end
136
137 chunks = payload/chip;
138 y = reshape(normalized,chip,chunks).'; % non-conjugate transpose
139
140 % find indices where inner product is maximum
141 yy = y*tribitSeq; % inner product
142 [~, correlated] = max(yy,[],2);
143 correlated = correlated - ones(chunks,1); % fix matlab indexing
144 % symbol error rate
145 %correlated_exp = textread('correlated.txt','%n');
146 %symerr = 100*numel(find((correlated == correlated_exp) == 0))/chunks;
147
```

```
% decode
if ~strcmp(BW,'4')

    % base change
    bin = dec2bin(correlated,4)';
    bin = str2num(reshape(bin,numel(bin),1));

    if ~strcmp(BW,'1+')
        % deinterleave
        bin = reshape(bin,col,row)';
        codedBits = reshape(bin,numel(bin),1);
    else
        codedBits = bin;
    end

    % coded bit error rate
    %codedBits_exp = textread('codedbits.txt','%n');
    %biterr = 100*numel(find((codedBits == codedBits_exp) == 0))/numel(bin)

    % viterbi decode w/ tail-biting, 2 iterations
    trellis = poly2trellis(constlen,codegen);
    tblen = 5*constlen;
    if ~strcmp(BW,'1+')
        vit = vitdec([codedBits;codedBits],trellis,tblen,'trunc','hard');
        %vit = vitdec(codedBits,trellis,tblen,'term','hard');
    else
        vit = vitdec([codedBits;codedBits],trellis,tblen,'trunc',...
            'hard',puncpat);
    end
    n = rate*numel(bin); % number of decoded bits
    bits = vit(n+1:end);

    % bit error rate
    %bits_exp = textread('bits.txt','%n');
    %biterr = 100*numel(find((bits == bits_exp) == 0))/n;
else
    % base change
    bin = dec2bin(correlated,2)';
    bits = str2num(reshape(bin,numel(bin),1));
end
```

A.3 Spatial-Temporal Equalizer

```
function [symbols, error, weightsOutput] = equalizer(rxsig, ...
       trainsig, initialWeights, resetWeights, eqMode, ...
       refTap, stepSize, lambda, delta1, M)
% Spatial-temporal adaptive 8-PSK equalizer using LMS or RLS algorithms
%
% function [symbols, error, weightsOutput] = equalizer(rxsig, ...
%       trainsig, initialWeights, resetWeights, eqMode, ...
%       refTap, stepSize, lambda, delta1, M)
% Inputs:
%   rxsig, the signal to be equalized
%   trainsig, the training sequence
%   initialWeights, initial tap weight vector
%   resetWeights, set to 1 to reset the weights
%   eqMode, set to 1 for LMS, else RLS
%   refTap, reference tap
%   stepSize, step size when using LMS
%   lambda, forgetting factor when using RLS
%   delta1, regularization parameter when using RLS
%   M, the number of inputs to the multichannel equalizer; set to
%       1 for single-channel (conventional temporal equalizer) operation.

% Equalizer settings
L = length(initialWeights); % number of tap weights

persistent weights
if(isempty(weights))
    weights = initialWeights + 0j;
end

% Initialize
k = zeros(L, 1) + 0j; % Gain vector (both LMS and RLS)
Delta = zeros(L, L) + 0j;  Delta(1:L+1:end) = delta1;  % inv. corr. mtx.
if resetWeights==1
    weights = initialWeights + 0j;
end

% input vector u(n)
for mm=1:M
    evalstr=['u' num2str(mm) '= zeros(L/M,1) + 0j;'];
```

```
    eval(evalstr);
end

delay = refTap - 1;
symbols = zeros(length(rxsig),1);
error = zeros(length(rxsig),1);
for n = 1:length(rxsig)

    % tapped delay line
    evalstr2='u=[';
    for mm=1:M
        evalstr=['u' num2str(mm) '=  [rxsig(n,mm); u' num2str(mm) ...
            '(1:L/M-1)];'];
        eval(evalstr);
        evalstr2 = [evalstr2 'u' num2str(mm) ';'];
    end
    evalstr2 = [evalstr2 '];'];
    eval(evalstr2);

    if n >= delay
        y = weights' * u;
        m = n - delay + 1;
        if n<=length(trainsig)
            % training mode
            d = trainsig(m);
        else
            % decision-directed mode
            d = pskdemod(y,8);
            d = exp(1j*2*pi/8*d);
        end
        e = d - y;  % symbol estimation error
        if eqMode==1
            % LMS
            k = stepSize*u;
        else
            % RLS
            k = Delta * u / (lambda + u'*Delta*u);
            Delta = 1/lambda * (Delta - k*u'*Delta);
        end
        weights = weights + k*conj(e);  % update weights
        symbols(m) = y; % note: last (delay-1) symbols not estimated
        error(m) = e;
    end
```

```
83 end
84 weightsOutput = weights;
```

A.4 Watterson Channel Simulator

```
1  function [y,a_i] = ChannelSimulator_v5(x,fs,model,K,fd,tau,gaindB,...
2      SNRdB,state,graph,response,angle0,angle1)
3  % [y,SNRret] = ChannelSimulator_v2(x,fs,model,K,fd,tau,gaindB,SNRdB,...
4  %                                  state,graph)
5  % implements & applies a time-varying channel using the model specified by
6  % K different paths, each of which have an fd Doppler measuarement,
7  % separated by tau ms, and have gains of gaindB.  The overall SNR is given
8  % by SNRdB.
9  %
10 % INPUT
11 %   x -> signal exciting the channel
12 %   fs ->sample rate of x
13 %   model -> string representing model type [Clarke,Watterson]
14 %   K -> number of differnt paths
15 %   fd -> Doppler measurment for each path
16 %   tau -> relative path delays
17 %   gaindB -> path gains
18 %   SNRdB -> SNR of channel output in dB
19 %   state -> seed for internal random number generators, if empty no seed
20 %            is provided (DEFAULT state = [])
21 %   graph -> plot the intermediate results of channel
22 %   M -> number of receive antennas
23 % OUTPUT
24 %   y -> signal output of channel simulator
25 %   SNRret -> measured SNR of channel
26 %
27 %  Version 1.1 RC 11.15.2006
28 %
29 % July, 2013 SGM added array response
30 % August, 2013 SGM added MRC gains
31
32 numArgs = 10;
33 if(nargin<numArgs)
34     graph = 0;
35 end
36 if(nargin<numArgs-1)
```

```
37      state = [];
38  end
39
40  %-------------------------------------------------------------------------
41  % Ver1: Initial release (11.03.2006)
42  % Ver1.1: Added a parameter for seeding the internal number generators
43  %          (11.15.2006)
44  % Ver2: Added different doppler measreuments for each path
45  %-------------------------------------------------------------------------
46
47  %=========================================================================
48  % Required functions that are not standard
49  % Matlab toolbox functions
50  %   interp() -> interpolates a signal
51  %   rand()   -> random number generator
52  %   randn()  -> Gaussian number generator
53  %   conv2()  -> 2-D convolution
54  %
55  % Self written
56  %   OptInt()       -> find optimal minimal sampling rate with easy
57  %                         upconversion
58  %   DopplerSpect() -> calculats the Doppler spectrum
59  %   interpMat()    -> diminsional interpolation of a matrix
60  %=========================================================================
61
62  %-------------------------------------------------------------------------
63  % Initialized the function
64  Ps = x(:)'*x(:)/length(x);
65  N0 = Ps/(10^(SNRdB/10));
66  if(size(x,2)==1)
67      x = x(:).';
68  end
69  lenX = length(x);
70  gain = 10.^(gaindB/10);
71
72  %-------------------------------------------------------------------------
73  % construct the basis channel vector and where the different taps
74  % representing the different paths will lie
75
76  % must account for the case where someone enters a delay of zero
77  if(tau(1)==0)
78      tau = tau(2:end);
79  end
```

```
80  if(K==1)
81      flen = 1;
82      h = 0;
83      tapNdx = 1;
84  else
85      flen = ceil(sum(tau)*1E-3*fs)+1;
86      h = zeros(flen,1);
87      tap = h;
88      tap(1)=1;
89      lasttap = 1;
90      for ii=1:length(tau)
91          tapspot = round(tau(ii)*1E-3*fs);
92          tap(lasttap+tapspot) = 1;
93          lasttap = lasttap+tapspot;
94      end
95      tapNdx = find(tap==1);
96  end
97  %-------------------------------------------------------------------------
98
99
100 %-------------------------------------------------------------------------
101 % Compute the Doppler for each individual tap and apply to said tap
102 H = [];
103 for ii=1:K
104     %---------------------------------------------------------------------
105     % Compute the appropriate spectrum
106     % determine an optimal intermidiate sample rate
107     fm = 32*fd(ii);
108     if(rem(fs,fm)==0)
109         ifs = fm;
110     else
111         ifs = OptInt(fs,fm);
112     end
113     [sd,fsDop] = DopplerSpect(model,fd(ii),ifs,graph);
114     [~,gpdel] = max(abs(sd));
115     %---------------------------------------------------------------------
116     %---------------------------------------------------------------------
117     % compute each tap in blocks and apply these as they are generated
118     trunc = gpdel;
119     % compute interpolation factor
120     up = fs/fsDop;
121
122     % generate white noise for each tap
```

```
123     % q is 2*K because it has both real and imag of each path
124     if(~isempty(state))
125         randn('state',state*342)
126     end
127     q = randn(2,ceil(lenX/up)+2*trunc);
128     if(graph)
129         fprintf('created random noise\n')
130         figure;plot(q.')
131     end
132
133     % shape to the desired spectrum
134     q = conv2(q,sd);
135     if(graph)
136         fprintf('shaped noise\n')
137         figure;plot(q.')
138     end
139     q = q(:,trunc:end-trunc);
140     if(graph)
141         figure;plot(q')
142     end
143
144     % concatenate with percent of overlap from previous block
145     %  and interpolate tot eh desired sample rate
146     if(graph)
147         fprintf('starting interpolation\n')
148         tic
149     end
150     %qsz1 = size(q)
151     %up
152     q = interpMat(q,up);
153     if(graph)
154         t1 = toc;
155         fprintf('Interpolation took %f sec\n',t1);
156     end
157     %qsz2 = size(q)
158
159     % Add new tap to channel STORAGE matrix and concatinate if needed
160     if ((size(H)==0) | (size(H,2)==size(q(:,1:lenX),2)))
161         H = [H;q(:,1:lenX)];
162     elseif(size(H,2)>size(q,2))
163         H = [H;q(:,1:size(H,2))];
164     elseif(size(H,2)<size(q,2))
165         H = [H;[q zeros(2,size(H,2)-size(q,2))]];
```

```
166     else
167         H = [H;q];
168     end
169 end
170 
171 % Get array response here for each path
172 M = size(response,1);       % number of rx antennas
173 A = zeros(length(h),M);
174 A(1,:) = response(:,angle0);     A(end,:) = response(:,angle1);
175 
176 % apply channel to the signal for this block
177 for jj=1:lenX-flen+1
178     xvec = x(jj:jj+flen-1);
179     %length(gain(:))
180     %size(H(1:2:end,jj))
181     %size(H(2:2:end,jj))
182     h(tapNdx) = gain(:).*(H(1:2:end,jj)+1j*H(2:2:end,jj));
183     % construct hM here with an intersting combo of h and array responses
184     % possibly through the use of transpose and kahtri-Rao products
185     % hM will be a flenxM matirx
186     % dimenstions will need to be worked out.
187     hMat = repmat(h,1,M).*A;
188     y(jj,:) = xvec*hMat;
189     %y(jj) = xvec*h;
190 end
191 
192 % add white noise of specified power
193 if(~isempty(state))
194     randn('state',state*751);
195 end
196 w = sqrt(N0/2)*(randn(size(y))+1j*randn(size(y)));
197 sig2_n = zeros(1,M);
198 SNRret = zeros(1,M);
199 a = zeros(1,M);
200 for mm = 1:M % number of rx antennas
201     sig2_n(mm) = w(:,mm)'*w(:,mm)/length(w);
202     a(mm) = Ps/sig2_n(mm);
203     SNRret(mm) = 10*log10(a(mm));
204 end
205 a_i = a/sum(a);
206 y = y + w;
207 if(graph)
208     figure;plot(y,'o')
```

```
end

return

%=========================================================================
% EXAMPLE INPUTS FOR THIS FUNCTION
% this example is equivalent to the ITU "good" condition.
% x = exp(j*2*pi/8*fix(8*rand(1,2000))); % input signal
% fd = 0.1; % Doppler measurement (Hz)
% fs = 2.4E3; % sample rate (Hz)
% K = 2; % number of paths
% tau = 0.5; % relative path delays (msec)
% gaindB = [0 -1]; % gain of relative paths (dB)
% model = 'Watterson'
% SNRdB = 15;
% graph = 1;
%=========================================================================
```

A.5 ALE3G Equalizer Comparison

```
% ALE3G comparison of diversity receivers
clear all;close all;clc

% simulation parameters
iter = 1000;
SNRdB = -20:15;%-20:20; % rx noise only
M = 4;

% equalizer parameters
nWeights = 24;      % 48,36,24,12 must be >= M*refTap and a multiple of 1:M
refTap = 6;         % 12,9,6,3 % nWeights/M;
eqMode = 0;         % RLS=0,LMS =1
lambda = 0.95;      % forgetting factor (RLS)
mu = 0.01;          % step size (LMS)
delta1 = 0.01;      % regularization parameter (RLS)
initialWeights = zeros(nWeights,1);
resetWeights = 1;

% array parameters
c = 299.79246;  % speed of light, km/ms
fc = 1.8;       % carrier freq, MHz
```

```
22
23 % channel parameters
24 baud = 2400;
25 fs = 4*baud;      % sample rate (Hz) % upsamp = 4
26 model = 'Watterson';
27 K = 2;
28 fd = [0.1 0.1];  % Doppler measurement (Hz)
29 tau = 0.5;       % relative path delays (msec)
30 gaindB = [0 -1]; % gain of relative paths (dB)
31 state = [];
32 graph = 0;
33 angle0 = 20; % this is the angle to use for MRC if gaindB(1) > gaindB(2)
34 angle1 = 80;
35
36 % initializations
37 lenSNR = length(SNRdB);
38 e1 = zeros(2432,iter);
39 e2 = zeros(2432,iter);
40 e3 = zeros(2432,iter);
41 mse1 = zeros(2432,iter);
42 mse2 = zeros(2432,iter);
43 mse3 = zeros(2432,iter);
44 berVec1 = zeros(lenSNR,M,iter);
45 berVec2 = zeros(lenSNR,M,iter);
46 berVec3 = zeros(lenSNR,M,iter);
47
48 for ii = 1:iter
49     % modulate
50     [bits_tx,tx,upsamp,syms] = ALE3Gmod('5');
51     train = syms(1:832);
52     lenTx = length(tx);
53     tx = cat(1,tx,zeros(upsamp+1,1)); % channel chops last upsamp+1 syms
54
55     for mm = 1:M
56         % more array parameters
57         M_vec = ones(1,mm-1);
58         el_r = [0 c/(fc*2).*M_vec];
59         el_r = cumsum(el_r);    % distance between each antenna
60         el_az = 0*el_r;
61         z = 0*el_r;
62
63         % create array manifold
64         [resp,az] = Omni_res(el_r,el_az,z,fc,180,0,0);
```

```
65
66          % initialize rx signal
67          rxWatterson = zeros(mm,lenTx);
68          for jj = 1:lenSNR
69
70              % channel and noise
71              [rxWatterson,a_i] = ChannelSimulator_v5(tx,fs,model,K,...
72                  fd,tau,gaindB,SNRdB(jj),state,graph,resp,angle0,angle1);
73
74              % baud sample
75              rx = downsample(rxWatterson,upsamp);
76
77              %%%% method 1: Joint spatial-temporal equalizer
78              % equalize
79              [y1,e1(:,ii),~] = equalizer(rx,train,initialWeights,...
80                  resetWeights,eqMode,refTap,mu,lambda,delta1,mm);
81              mse1(:,ii) = e1(:,ii).^2;
82
83              % demodulate
84              bits_rx1 = ALE3Gdemod('5',y1,0);
85              [~,berVec1(jj,mm,ii)] = biterr(bits_rx1,bits_tx);
86
87
88              %%%% method 2: MRC followed by single-channel equalizer
89              % maximal ratio combining
90              wtMRC = resp(:,angle0);
91              wtRep = repmat(wtMRC,1,lenTx/upsamp);
92              a_iRep = repmat(a_i,lenTx/upsamp,1);
93              rx2 = a_iRep.*rx;
94              rxMRC =  sum(conj(wtRep).*rx2.',1)./sum(wtMRC.*conj(wtMRC),1);
95
96              % equalize
97              [y2,e2(:,ii),~] = equalizer(rxMRC,train,initialWeights,...
98                  resetWeights,eqMode,refTap,mu,lambda,delta1,1);
99              mse2(:,ii) = e2(:,ii).^2;
100
101             % demodulate
102             bits_rx2 = ALE3Gdemod('5',y2,0);
103             [~,berVec2(jj,mm,ii)] = biterr(bits_rx2,bits_tx);
104
105
106             %%%% method 3: EGC followed by single-channel equalizer
107             % equal gain combining
```

```
108             rxEGC =  sum(conj(wtRep).*rx.',1)./sum(wtMRC.*conj(wtMRC),1);
109
110             % equalize
111             [y3,e3(:,ii),~] = equalizer(rxEGC,train,initialWeights,...
112                 resetWeights,eqMode,refTap,mu,lambda,delta1,1);
113             mse3(:,ii) = e3(:,ii).^2;
114
115             % demodulate
116             bits_rx3 = ALE3Gdemod('5',y3,0);
117             [~,berVec3(jj,mm,ii)] = biterr(bits_rx3,bits_tx);
118         end
119     end
120     fprintf('Iteration %d of %d complete.\n',ii,iter);
121 end
122
123 % calculate MSE across all independent trials
124 mse1av = mean(mse1,2);
125 mse2av = mean(mse2,2);
126 mse3av = mean(mse3,2);
127
128 % calculate BER across all independent trials
129 ber1 = mean(berVec1,3);
130 ber2 = mean(berVec2,3);
131 ber3 = mean(berVec3,3);
132
133 % plotting
134 figure,plot(y1,'x');
135 %title('Joint Spatial-Temporal Equalizer Raw Symbols')
136 xlabel('In-Phase'), ylabel('Quadrature')
137 axis([-1.2 1.2 -1.2 1.2])
138 figure,plot(y2,'x');
139 %title('Single-Channel Equalizer Raw Symbols')
140 xlabel('In-Phase'), ylabel('Quadrature')
141 axis([-1.2 1.2 -1.2 1.2])
142 % NOTE: equalizer raw syms constellations are for a single sample at a
143 % single SNR value and for a single # of diversity branches
144
145 figure,plot(abs(mse1av(1:832)));
146 hold on,plot(abs(mse2av(1:832)),'r');
147 ylabel('Mean Squared Error')
148 xlabel('Training Symbols')
149 legend('Joint spatial-temporal equalizer','MRC + single-channel equalizer')
150 %title('Learning curves for both diversity receivers')
```

```
% NOTE: learning curve are for a single SNR value and single # of diversity
% branches, but averaged over independent trials

figure,semilogy(SNRdB,ber3,':','LineWidth',2.5)
xlabel('Signal-to-Noise Ratio, dB')
ylabel('Bit Error Rate')
%title('BER vs SNR for both diveristy receivers')
%xlim([-20 0])
%ylim([0.004 1])
grid on
hold on, semilogy(SNRdB,ber2,'--','LineWidth',2.5)
semilogy(SNRdB,ber1,'LineWidth',2.5)
legend('EGC + single-channel equalizer M=1',...
    'EGC + single-channel equalizer M=2',...
    'EGC + single-channel equalizer M=3',...
    'EGC + single-channel equalizer M=4',...
    'MRC + single-channel equalizer M=1',...
    'MRC + single-channel equalizer M=2',...
    'MRC + single-channel equalizer M=3',...
    'MRC + single-channel equalizer M=4',...
    'Joint spatial-temporal equalizer M=1',...
    'Joint spatial-temporal equalizer M=2',...
    'Joint spatial-temporal equalizer M=3',...
    'Joint spatial-temporal equalizer M=4')
```

Bibliography

[1] M.W. Chamberlain and W.N. Furman. HF data link protocol enhancements based on STANAG 4538 and STANAG 4539, providing greater than 10 kbps throughput over 3 khz channels. In *HF Radio Systems and Techniques, 2003. Ninth International Conference on (Conf. Publ. No. 493)*, pages 64–68, 2003.

[2] M.W. Chamberlain, W.N. Furman, L. F. Palum, and G. R. Robertson. Performance of US MIL-STD-188-141b appendix c data link protocols. In *HF Radio Systems and Techniques, 2000. Eighth International Conference on (IEE Conf. Publ. No. 474)*, pages 145–149, 2000.

[3] Frank's Web Space: Radio Communications. http://www.frankswebspace.org.uk /scienceandmaths/physics/physicsgce/radiocomms.htm, 2007.

[4] LigiaChira Cremene, Nicolae Crisan, and Marcel Cremene. An adaptive combiner-equalizer for multiple-input receivers. In Tarek Sobh, Khaled Elleithy, and Ausif Mahmood, editors, *Novel Algorithms and Techniques in Telecommunications and Networking*, pages 385–390. Springer Netherlands, 2010.

[5] Y. Erhel. A blind spatio temporal equalization operating on a polarization sensitive array. *13th European Signal Processing Conference*, 2005.

[6] A. Goldsmith. *Wireless Communications*. Cambridge University Press, 2005.

[7] R.P. Gooch and B.J. Sublett. Joint spatial and temporal equalization in a decision-directed adaptive antenna system. In *Signals, Systems and Computers, 1988. Twenty-Second Asilomar Conference on*, volume 1, pages 255–259, 1988.

[8] J.S. Hammerschmidt, C. Drewes, and A.A. Hutter. Adaptive space-time equalization for mobile receivers. In *Acoustics, Speech, and Signal Processing, 2000. ICASSP '00. Proceedings. 2000 IEEE International Conference on*, volume 5, pages 3013–3016 vol.5, 2000.

[9] S.S. Haykin. *Adaptive filter theory*. Prentice-Hall information and system sciences series. Prentice Hall, 2002.

[10] N. Ishii and R. Kohno. Spatial and temporal equalization based on an adaptive tapped-delay-line array antenna. In *Personal, Indoor and Mobile Radio Communications, 1994. Wireless Networks - Catching the Mobile Future., 5th IEEE International Symposium on*, volume 1, pages 232–236, 1994.

[11] E.E. Johnson. Third-generation technologies for HF radio networking. In *Military Communications Conference, 1998. MILCOM 98. Proceedings., IEEE*, volume 2, pages 386–390, 1998.

[12] E.E. Johnson. Simulation results for third-generation HF automatic link establishment. In *Military Communications Conference, 1999. MILCOM 99. Proceedings., IEEE*, 1999.

[13] E.E. Johnson, E. Koski, W.N. Furman, M. Jorgenson, and J. Nieto. *Third-Generation and Wideband HF Radio Communications*. Artech House mobile communications series. Artech House, 2012.

[14] E.N. Koski. STANAG 4538 implementation and field testing lessons learned. *Ninth International Conference on HF Radio Systems and Techniques*, pages 256–261(5).

[15] Erik Lindskog, A. Ahlen, and M. Sternad. Combined spatial and temporal equalization using an adaptive antenna array and a decision feedback equalization scheme. In *Acoustics, Speech, and Signal Processing, 1995. ICASSP-95., 1995 International Conference on*, volume 2, pages 1189–1192 vol.2, 1995.

[16] MATLAB. *version 8.1.0.604 (R2013a)*. The MathWorks Inc., Natick, Massachusetts, 2013.

[17] J. McGehee. Multi-site spatially diverse demodulation of HF propagated signals. In *Military Communications Conference, 2008. MILCOM 2008. IEEE*, pages 1–6, 2008.

[18] MIL-STD-188-141B. *Military Standard - Interoperability and Performance Standards for Medium and High Frequency Radio Systems*. US Dept of Defense, March 1999.

[19] J.G. Proakis and M. Salehi. *Digital Communications 5th Edition*. McGraw Hill, 2007.

[20] Recommendation ITU-R F.1487. *Testing of HF Modems with Bandwidths of up to about 12 kHz using ionospheric Channel Simulators*. International Telecommunication Union, Radiocommunication Sector, Geneva, 2000.

[21] STANAG 4538. *Technical Standards for an Automatic Radio Control System for HF Communications Links*. NATO Standarization Agency, February 2009.

[22] Lin Sun, Ruo Li, and Tian Zhou. Improvement of passive time reversal communications using spatial diversity equalization. In *Instrumentation, Measurement, Computer, Communication and Control (IMCCC), 2012 Second International Conference on*, pages 256–261, 2012.

[23] M.A. Wadsworth. Performance simulation of HF subnetworks employing third generation HF link establishment protocols. In *Frequency Selection and Management Techniques for HF Communications (Ref. No. 1999/017), IEE Colloquium on*, pages 13/1–13/6, 1999.

[24] C. Watterson, J. Juroshek, and W.D. Bensema. Experimental confirmation of an HF channel model. *Communication Technology, IEEE Transactions on*, 18(6):792–803, 1970.

[25] Fan Zhang, Benxiong Huang, Lai Tu, and Jian Zhang. Simulation and evaluation of an HF email network. In *Military Communications Conference, 2006. MILCOM 2006. IEEE*, pages 1–5, 2006.